REVISTAMATĒRIA V.31
ISSN 1517-7076 articles e20260116, 2026

Optimizing concrete performance through fine aggregate selection: experimental study and desirability-based modeling

Nécira Brahim[1,2], Allout Naas[1,3], Guettala Salah[2,4], Chetbani Yazid[5], Guettala Salim[1,2]

[1]Ziane Achour University of Djelfa, Faculty of Science and Technology, Civil Engineering Department. Djelfa, Algeria.

[2]Mohamed Khider University of Biskra, Faculty of Science and Technology, Laboratory of Civil Engineering Research. Biskra, Algeria.

[3]Ziane Achour University of Djelfa, Faculty of Science and Technology, Laboratory of Civil Engineering and Sustainable Development. Djelfa, Algeria.

[4]Houari Boumediene University of Science and Technology, Faculty of Civil Engineering. Algiers, Algeria.

[5]Scientific and Technical Research Center for Physico-Chemical Analyses. Tipaza, Algeria.

e-mail: b.necira@univ-djelfa.dz, n.allout@univ-djelfa.dz, salah.guettala@usthb.edu.dz, chetbani.yazid92@gmail.com, guettalasalim@yahoo.com, s.guettala@univ-djelfa.dz

ABSTRACT

This study applies mixture design, ANOVA, and desirability function analysis to optimize concrete performance with river (RS), crushed (CS), dune (DS) sands, and their combinations. Experimental validation confirms the reliability, practical applicability, and sustainability of optimized mixes, while highlighting key property relationships. Study optimized concrete mixes and developed predictive models using a multi-objective desirability approach. Twenty-one mixtures with varying RS, CS, and DS were designed via a three-factor, five-level simplex lattice method. Key properties including slump, 7 and 28-day compressive (CS) and flexural (FS) strengths, capillary absorption, and UPV were measured. ANOVA and statistical modeling in Design-Expert13 validated factor significance and interactions, enabling reliable mathematical models to predict concrete performance. ANOVA results showed strong predictive performance (R2 = 0.80–0.91). RS improves workability, while moderate amounts of CS and DS sands enhance strengths and reduce open porosity. Best 28-day CS (36 MPa) was recorded for the mix consisting of 0.4RS+0.6CS. Ternary mix M10 (20%RS+60%CS+20%DS) achieved the highest 28-day CS, though excessive dune sand (>40%) decreases performance. Model predictions deviated less than 9% from experiments, confirming reliability. Significant correlations (R2>0.91) among CS, open porosity, density, UPV, and dynamic elasticity modulus enable non-destructive assessment. Local sands (CS, DS) are viable sustainable alternatives to RS.

Keywords: Concrete; Desirability-based modeling; Fine aggregate types; Optimization; Physico-mechanical properties.

1. INTRODUCTION

The construction industry is under increasing pressure to find viable alternatives to river sand (RS) due to supply problems caused by rapid infrastructure expansion in developing nations. Construction is where RS is most commonly employed. Crushed sand (CS) and dune sand (DS) are two alternatives to RS that have recently gained popularity because to concerns about resource depletion, environmental implications, and cost [1, 2]. The concept of green concrete encompasses a set of methods and materials aimed at reducing environmental impact [3–5], as well as minimizing the environmental burden resulting from resource extraction and depletion [6]. In this light, there are monetary and ecological advantages to making use of quarry dust as a by-product of the concrete industry. Because of its high fines content (10–15%), fine-rich CS is an environmentally friendly. Fines substantially influence the development of strengths and accelerate hydration during early stages [7, 8]. Additionally, their binding activity facilitates the formation of carbo-aluminates [8, 9]. To improve adhesion paste-aggregates, fines that are similar to limestone aggregates are used [10]. Strong concrete is a result of good adherence [11, 12]. An epitaxial aureole, formed by the reaction of cement with limestone particles, encircles the aggregate and gradually improves the paste-aggregate bond [13]. The writers go on to speculate that the angular shape, fineness of CS, limestone nature, and granulometry are responsible for this enhanced compactness.

Corresponding Author: Guettala Salim Received on 05/02/2026 Accepted on 03/06/2026

DOI: https://doi.org/10.1590/1517-7076-RMAT-2026-0116

Because of its massive size and sharp angles, CS improves the mechanical characteristics of concrete [14, 15]. You can use CS with up to 15% fines without worrying about mechanical strengths being badly affected [16]. Several studies [17, 18] have analyzed the characteristics of quarry dust and evaluated its possible applicability as a partial substitute for RS in concrete. The incorporation of quarry dust in concrete has been reported to contribute to the utilization of industrial by-products, a reduction in RS consumption, and, under certain conditions, improvements in strength-related properties and workability [19, 20]. The feasibility of using alternative fine aggregates in concrete has been widely investigated. AKROUT *et al*. [21] compared CS-based concretes to RS-based ones, and conducted experiments to determine the effect of CS proportioning on compressive strength and workability. Their findings showed that, while concretes produced with CS generally exhibited lower properties than those incorporating RS, the overall performance remained comparable. When rock flour was partially substituted for RS in concrete, RAO *et al*. [22] found that the compressive strength of the mixture was increased. The approach of utilizing quarry-derived sand (CS) as an alternative fine aggregate is based on the hardness and density of its parent material, granite, which provides suitable mechanical performance. Incorporating quarry fines in concrete has been associated with potential improvements in compressive strength, durability, strength development, workability, and cost-effectiveness. Compressive strength is an essential characteristic for assessing the quality of concrete in structural applications; such improvements are particularly relevant when evaluating alternative fine aggregates. Researchers MENADI *et al*. [16] looked at how CS fines affected the concrete's mechanical and physical characteristics. The impact of limestone particles on the strength of concrete was the subject of the investigation, taking into account four distinct cement types while keeping the water-to-cement ratio constant. The findings demonstrated that concrete strength may be adequately preserved with CS fines content up to 15%. REDDY and SATYANARAYANA REDDY [23] similarly observed improved compressive strength with rock flour as a partial RS replacement. ILANGOVANA *et al*. [24] reported that concrete containing quarry rock dust exhibited comparable or slightly higher strength than conventional mixes. HAMEED and SEKAR [25] evaluated crushed stone dust's impact on flexural strength, noting increases at lower replacement levels, while higher proportions of crusher dust led to reductions in strength. POON *et al*. [26] discovered that the compressive strength of ordinary, intermediate, and high strength concretes produced with mixtures containing partial proportions of CS and RS was consistently higher across all test ages. Collectively, these studies indicate that CS may be a viable alternative to RS, its mechanical performance depending on the material properties, replacement proportions, and the concrete mix design. The Algerian Sahara contains extensive DS deposits that can be economically and environmentally valorized in concrete production, offering a local alternative to scarce conventional aggregates and high transportation costs. The use of DS in the production of both traditional and modern concrete has recently attracted the attention of numerous researchers [1, 2, 27–38]. High water absorption, very tight granularity, and extreme fineness are the DS defining characteristics [39]. The DS grains are round and almost homogeneous in size [40]. A drop in strengths is possible if the DS rate is increased in the concrete [41, 42]. It is possible to optimize the RS particle size distribution using DS [43]. Hence, it's important to use locally sourced materials and available by-products in the concrete mix. So that we can address the environmental, economic, and technical issues, we must do this. A number of studies have experimentally assessed how various combinations of sand kinds affect the characteristics of self-compacting concrete (SCC) [1, 2, 44, 45]. BEDERINA *et al*. [43] examined the use of locally abundant sand in sandcrete production. Their findings indicated that optimizing the particle size distribution by blending two local sands in controlled proportions enhanced workability, compactness, and mechanical strength. In concrete mix design, aggregate grading and fineness are key parameters that significantly affect the concrete properties. BROUWERS and RADIX [46] reported that using fine sand in concrete mixes can significantly improve mechanical performance, stability, and flowability by adjusting the particle size distribution. KAY *et al*. [47] studied DS's potential as a fine aggregate in concrete and found it to be a useful ingredient. BOUZIANI *et al*. [48–52] examined the characteristics of fluid concrete that contained DS. Their results indicated that an optimal proportion of DS allows for satisfactory properties of fluid concrete, both in the fresh and hardened states. BOUZIANI [50] applied a mixture design approach to investigate how DS, RS, and CS influence both fresh and hardened characteristics of SCC. The study highlighted that achieving optimal performance requires careful balance among the three sand types: flowability, passing ability, and stability can be maintained through appropriate proportions, while compressive strength tends to increase with higher CS content and decrease with higher DS content. RMILI *et al*. [53] investigated the incorporation of DS, RS, and CS in SCC. The study showed that combining different sand types can enhance workability, while the inclusion of DS increases viscosity but may reduce mechanical strength. In contrast, CS-RS combinations improve both compressive and tensile strengths, with optimized blends providing the best overall SCC performance. In order to conduct the fewest number of laboratory tests feasible, it is essential to use an analytical method that can account for the effect of each parameter independently and in combination with other parameters on the features under study. Mix design provides an effective method for simplifying experimental programs and experimentally modeling material behavior [54]. Although it is widely used in cement research due to its simplicity and speed of application [37, 38, 55], has seen minimal application in the sands field, especially on the SCC as discussed by BOUZIANI [50] and SAHRAOUI and BOUZIANI [56]. Predictive modeling plays a crucial role in optimizing concrete mix design. According to TIPU *et al*. [57], accurate prediction of the compressive strength of high performance concrete is essential for mix design optimization and ensuring structural reliability. Predictive modeling approaches enable the efficient optimization of concrete mixtures, thereby improving structural performance while significantly reducing the dependence on extensive, time-consuming, and costly laboratory testing programs [58–60]. This experimental study examines the workability of concrete in its fresh state, as well as the flexural and compressive strengths after 7 and 28 days, the open porosity at 28-day estimated by the initial amount of water absorbed after 1 hour per unit surface, and the dynamic elasticity modulus of the hardened concrete after 28-day, which was estimated by the ultrasonic pulse velocity. It aims to assess and model the impact of various fine aggregate types and proportions with varying morphologies and locally available sources (RS, CS, DS, and their binary and ternary combinations). This study uses a multi-objective approach to predict the best formulations that combine these characteristics. It incorporates statistical modeling using an ANOVA analysis of variance in conjunction with a three-factor mix design. Furthermore, there appears to be a lack of research on the experimental validation of the prediction models created. To fill this gap, this study employs a rigorous optimization technique and then uses precise experimental validation to prove the performance of the optimized formulations. At last, certain connections between the many mechanical and physical characteristics of concrete have been discovered. The novelty is not in studying RS, CS, and DS individually, but in: their combined multi-objective optimization, interaction-based modeling, experimental validation of predictions, and integration of performance prediction with sustainability goals. This study is distinguished from prior mixture design and optimization research by several integrated methodological and practical advances, rather than treating mixture design as an isolated statistical exercise: fully integrated multi-objective optimization framework, explicit modeling of ternary interactions (RS-CS-DS), coupling statistical modeling with experimental validation, development of high-quality predictive models across multiple responses, establishment of strong inter-property correlations for non-destructive evaluation, and focus on locally available materials within a sustainability framework.

2. EXPERIMENTAL PROCEDURE

2.1. Identification of utilized materials

The cement adopted in this investigation was CEM II/B 42.5, with a specific density of 3150 kg/m^3, an apparent density of 1100 kg/m^3, and a Blaine specific surface area of 4180 cm^2/g. The chemical and mineralogical compositions of the cement are reported in Table 1, respectively. The mineralogical phases were determined using the Bogue calculation method [61]. Mixing water of potable quality was used throughout the experimental program. Three different types of sand collected from the Djelfa region were employed, namely river sand (RS), crushed sand (CS), and dune sand (DS), with maximum grain sizes of 3 mm, 3 mm, and 0.63 mm, respectively. Microscopic observations were performed at 40× magnification in addition to EDX analysis on the examined sands, as shown in Figure 1. The results reveal that both DS and RS are predominantly siliceous, while CS mainly consists of limestone. Regarding particle morphology, RS exhibits a generally spherical shape, CS particles are angular, and DS particles display a rounded spherical geometry. The particle size distributions and the main physical

Table 1: Chemical and mineralogical analysis of the cement (in %).

CHEMICAL ANALYSES		MINERAL CONTENT OF CEMENT	
CaO	62.78	C_3S	55.41
SiO_2	17.49		
SO_3	2.38	C_2S	13.65
Al_2O_3	4.51		
Fe_2O_3	3.02	C_3A	2.25
MgO	2.15		
K_2O	0.64	C_4AF	14.83
Na_2O	0.05		
LOI	8.10		

Table 2: Main physical features of the three types of sands and gravels.

FEATURES	RS	DS	CS	G 3.15/8	G 8/16
Coefficient of absorption (%)	0.25	3.71	6.53	0.47	0.47
Specific density (kg/m^3)	2500	2760	2630	2610	2610
Apparent density (kg/m^3)	1440	1450	1415	1330	1380
Finesses modulus (FM)	2.79	0.92	2.93	-	-
Fines < 80 µm (%)	0.65	0.24	5.04	-	-
Los Angeles coefficient (%)	-	-	-	24.50	24.00
Sand equivalent (%)	81.00	83.30	79.40	-	-

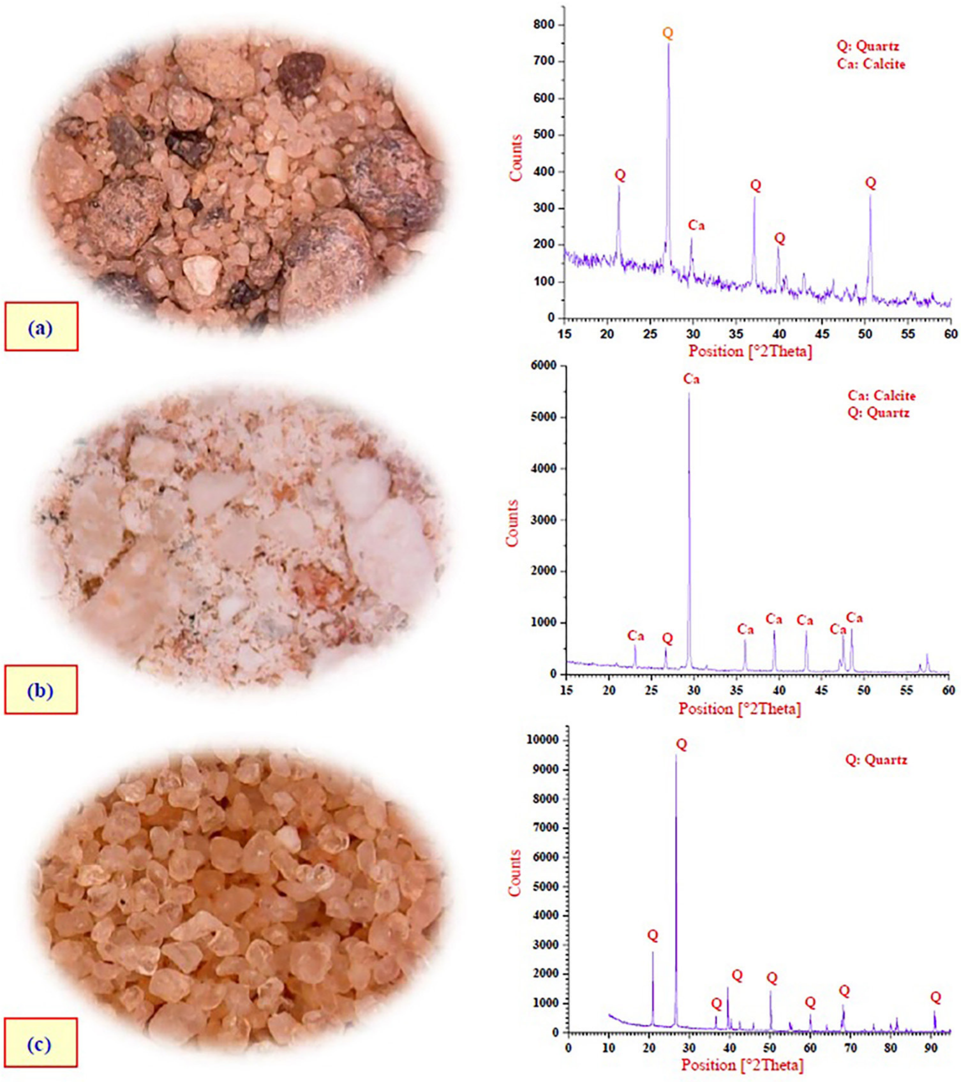

Figure 1: Microscopic observations (40× magnification) and EDX analysis of the investigated sands: (a) RS, (b) CS, and (c) DS.

properties of the three sands are illustrated in Figure 2 and summarized in Table 2, respectively. In addition, two gravel fractions (3.15/8 mm and 8/16 mm), also obtained from the Djelfa region, were incorporated. Table 2 and Figure 2 also provide their physical characteristics and grading curves.

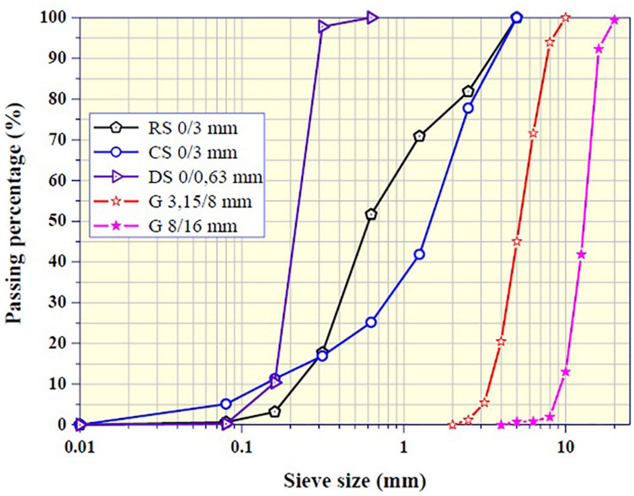

Figure 2: Particle size distribution curves of sands and gravels.

2.2. Mix design

An effective method for managing variability, optimizing product and formulation development, and exploring new possibilities is the mixture design. In doing so, it is possible to optimize formulations, save resources, study interactions, and produce insightful data that may be used to enhance products and processes. Statistical modeling techniques can be used to ascertain the proportional importance of significant mixture qualities and their interrelated effects on pertinent features. All variables in this study stand for mixture component proportions. Because all of the proportions that came before it must always add up to 1, the final percentage of each component is obtained by summing all the corresponding proportions. The design process is affected by the interdependence of the components in this mixed scenario [62]. A five-level, three-factor simplex-lattice mixed design was employed to evaluate the effect of RS, CS, and DS on the characteristics of concrete. The number of potential permutations (N) can be expressed as follows: where: L is levels number; F is factors number.

$$N^{L}_{F+L-1} = \frac{(F+L-1)!}{(L)!(F-1)!} \tag{1}$$

The number of combinations to be analyzed is $N = 21$, with three factors and five levels. Mix design employs unique graphical representations compared to conventional experimental designs. An equilateral triangle is adopted to represent the combined effect of the three factors. Statistical models outlining the many effects of factors and their binary and ternary permutations on a given feature can be constructed using this method. Three interconnected factors (RS = A, CS = B, and DS = C) and five levels made up the second-degree polynomial model. A description of the model is as follows:

$$Y = I_1 \times A + I_2 \times B + I_3 \times C + I_{12} \times (A.B) + I_{13} \times (A.C) + I_{23} \times (B.C) \tag{2}$$

Where: model's coefficients are (I_1, I_2, I_3, I_{12}, I_{13}, I_{23}); the response is (Y).

The effects of the studied factors and their interactions were quantified through model coefficients. Since these coefficients are not known in advance, they were estimated from the experimental results using a least-squares regression method. The variance of each coefficient was calculated from the residuals in order to evaluate the statistical significance of the corresponding model terms [54, 62]. Design-Expert software (version 13) was implemented for modeling of data and statistical analysis. Iso-response curves (ternary contour plots) were generated to illustrate the relationships among the three factors and their combined influence on the studied responses.

2.3. Formulation approach

Concrete mix design aims to determine the optimal proportions of the constituent materials in order to achieve both adequate mechanical strength and satisfactory workability. Several approaches are available for concrete proportioning; however, this study adopted a less commonly used approach known for its high accuracy, namely

Table 3: Compositions of the investigated concrete mixes and proportions of factors.

MIX	W l/m³	C kg/m³	W/C RATIO	FACTORS PRO-PORTIONS			RS kg/m³	CS kg/m³	DS kg/m³	G 3.15/8 kg/m³	G 8/16 kg/m³
				RS	CS	DS					
M 1	208	370		0	0	1	0	0	508.00		
M 2	206	366		0	0.2	0.8	0	102.36	409.44		
M 3	204	362		0	0.4	0.6	0	206.24	309.36		
M 4	202	358		0	0.6	0.4	0	311.64	207.76		
M 5	200	354		0	0.8	0.2	0	418.56	104.64		
M 6	198	350		0	1	0	0	527.00	0		
M 7	206	366		0.2	0	0.8	101.32	0	405.28		
M 8	204	362		0.2	0.2	0.6	102.08	102.08	306.24		
M 9	202	358		0.2	0.4	0.4	102.84	205.68	205.68		
M 10	200	354	0.56	0.2	0.6	0.2	103.60	310.80	103.60	448	832
M 11	198	350		0.2	0.8	0	104.36	417.44	0		
M 12	204	362		0.4	0	0.6	202.08	0	303.12		
M 13	202	358		0.4	0.2	0.4	203.60	101.80	203.60		
M 14	200	354		0.4	0.4	0.2	205.12	205.12	102.56		
M 15	198	350		0.4	0.6	0	206.64	309.96	0		
M 16	202	358		0.6	0	0.4	302.28	0	201.52		
M 17	200	354		0.6	0.2	0.2	304.56	101.52	101.52		
M 18	198	350		0.6	0.4	0	306.84	204.56	0		
M 19	200	354		0.8	0	0.2	401.92	0	100.48		
M 20	198	350		0.8	0.2	0	404.96	101.24	0		
M 21	198	350		1	0	0	501.00	0	0		

the B. Scramtaiv approach. The fundamental idea behind this approach is that the volume of the compacted concrete mix is equal to the total absolute volume of all ingredients contained in 1 m^3 [63]. The concrete was designed to achieve an average 28-day compressive strength of 32.5 MPa, with a workability corresponding to the plastic consistency class, characterized by a slump ranging from 50 to 90 mm. The workability of the material was evaluated by carrying out a slump test using the Abrams cone, in accordance with the guidelines of standard NF P 18-451 [64]. In all mixtures, the water-to-cement ratio (*w/c*) was fixed at 0.56, with A = 0.6 and a maximum aggregate size (D_{max}) of 16 mm. Both the 3.15/8 mm and 8/16 mm crushed gravel fractions were incorporated at proportions of 35% and 65%, respectively, of the total coarse aggregate volume. A constant *w/c* ratio of 0.56 was intentionally maintained in all mixtures to ensure a controlled and comparable experimental framework. The constant *w/c* ratio improves the validity of comparisons and the robustness of the predictive models. Table 3 summarizes the concrete mix compositions that were investigated and proportions of factors.

2.4. Samples preparation and tests performed

For this study, a grand total of twenty-one different concrete mixtures were mixed. After mixing and casting into molds, the samples were placed in the laboratory for 24 hours with plastic sheets covering them to prevent moisture loss. Upon demoulding, all specimens were cured in lime-saturated water at a controlled temperature of (20 ± 2°C) until testing. The second step involved the determination of the concrete density at 28 days in accordance with the NF P18-459 standard [65], prior to conducting the mechanical tests. Mechanical strength tests were performed at 7 and 28 days on six specimens, and the reported values correspond to the average of the measured results [63]. All tests were carried out under controlled laboratory conditions (T = 20 ± 2°C and RH = 45 ± 10%). Prismatic samples used have dimensions of (10 × 10 × 40) cm^3 to determine the flexural strength in accordance with EN 12390-5:2012 [66].

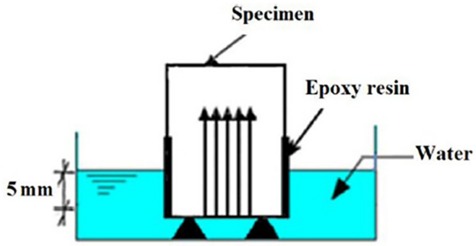

Figure 3: Experimental setup for capillary absorption testing.

Figure 4: Ultrasonic testing device for evaluating wave velocity.

The samples used were cubic in shape and measured (10 × 10 × 10) cm^3 for the capillary water absorption test at 28 days (Figure 3), as well as for compressive strength and ultrasonic pulse velocity (UPV) tests at 28 days (Figure 4), following the recommendations of AFPC-AFREM [67], EN 12390-3:2012 [68], and ASTM C597-02 [69], respectively. Sorptivity measurement provides a simple and effective method for characterizing the water absorption kinetics of concrete. A higher capillary absorption indicates an increased susceptibility of concrete to rapid liquid ingress. Prior to the initial capillary absorption (initial sorptivity) measurements, specimens were preconditioned according to the AFPC-AFREM procedure [67].

The samples were subsequently placed in a drying oven for 24 hours to reach thermal equilibrium, ensuring that the relative mass difference between two consecutive measurements did not exceed 1%, as recommended. Specimens were covered with resin on their side surfaces after drying to stop water from evaporating and seeping in during testing. The capillary absorption test was then conducted by immersing the specimens in water to a maximum depth of 5 mm. Water uptake was determined by monitoring the mass variation of the specimens over time. Prior to each weighing, the water film adhering to the bottom surface was carefully removed using absorbent paper [70]. Water absorbed volume per unit surface area after one hour was selected as the parameter representing the maximum density of capillaries within the concrete surface layer, as these capillaries are the most active in water transport [70, 71]. The initial water absorption coefficient after a suction time of one hour is expressed as: IA = Δm/A ($kg.m^{-2}.h^{-1/2}$). In the third stage, the open porosity of the twenty-one concrete mixtures was determined at 28 days in accordance with reference [70]. The open porosity after one hour of capillary suction was calculated as the ratio between the quantity of water absorbed per unit surface area (Δm/A) and the product of water density (β) and the height of the capillary rise (h), as expressed in Equation 3:

$$\varepsilon\ (\%) = ((\Delta m/A) / \beta \times h) \times 100\% \tag{3}$$

With ε: is the open porosity (%); Δm/A: represents the water absorbed amount per unit surface area after 1 h ($kg.m^{-2}.h^{-1/2}$); β: water density (10^3 $kg.m^{-3}$); and h: height of capillary imbibitions front (5 $cm.h^{-1/2}$, equivalent to 0.050 $m.h^{-1/2}$). Subsequently, the dynamic elasticity modulus was evaluated at 28 days for the same concrete mixtures in accordance with reference [69]. The dynamic elasticity modulus (E_d) was determined by Equation 4:

$$E_d = (v^2 \times \rho/g) \times 10^{-2} \tag{4}$$

With E_d: is the dynamic elasticity modulus (GPa); V: the ultrasonic pulse velocity (m.s^{-1}); ρ: the concrete density (kg/m^3); and g: gravitational force (9.81 m.s^{-2}).

3. RESULTS AND DISCUSSIONS

The results obtained from the characterization tests performed on the 21 concrete mixtures are presented in Table 4. On the basis of the experimental results, mathematical models were established to describe the influence of RS, CS, and DS, as well as their binary and ternary interactions, on each investigated response.

These models were developed to predict the slump, flexural strength (F_S) at 7 and 28 days, compressive strength (C_S) at 7 and 28 days, the water absorbed amount per unit surface after 1 hour at 28 days (Δm/A), and the ultrasonic pulse velocity at 28 days (V) of the studied concrete. High correlation coefficients were considered indicative of the reliability and adequacy of the proposed models.

Analysis of variance (ANOVA) was employed to analyze the experimental results and to evaluate the adequacy of the developed models. This statistical approach enables the assessment of the relative influence of the input factors on the variability of the measured responses [72, 73]. As reported by BERTINETTO *et al*. [74], ANOVA identifies the significance of differences among treatments by partitioning the total variance into contributions associated with individual factors and their interactions. This decomposition makes it possible to determine whether the observed variations are attributable to random effects or to statistically significant influences. Factors were deemed statistically significant if their p-values were less than 0.05, since a significance level of α = 0.05 was used in this investigation, which corresponds to a 95% confidence interval [75]. The statistical parameters evaluated through ANOVA are presented in Table 5. The three components A (RS),

Table 4: Outcomes of the experimental program.

MIX	SLUMP (mm)	DENSITY AT 28-DAY ρ kg/m³	STRENGTHS AT 7-DAY (MPa)		STRENGTHS AT 28-DAY (MPa)		QUANTITY OF WATER ABSORBED Δm/A kg.m⁻².h⁻¹ᐟ²	UPV V m/s
			FLEXURAL Fs	COMPRESSIVE Cs	FLEXURAL Fs	COMPRESSIVE Cs		
M 1	50	2390.00	3.00	17.30	3.80	21.00	6.02	3010
M 2	50	2371.00	3.10	18.50	4.00	22.30	5.81	3037
M 3	70	2354.00	3.90	22.80	5.00	27.50	4.45	3136
M 4	60	2336.00	4.20	24.50	5.90	32.70	3.08	3219
M 5	50	2318.00	4.00	23.60	5.70	31.50	3.45	3199
M 6	50	2300.00	3.80	22.70	5.60	31.00	3.52	3190
M 7	50	2357.68	3.20	18.60	4.00	22.50	5.70	3036
M 8	60	2339.68	3.70	22.00	4.80	26.80	4.59	3120
M 9	50	2321.68	4.20	24.50	5.60	31.20	3.50	3190
M 10	50	2303.68	4.50	26.00	6.30	34.70	2.68	3250
M 11	50	2285.68	4.30	25.00	6.00	33.30	2.94	3225
M 12	70	2325.36	4.00	23.90	5.20	28.80	4.06	3160
M 13	60	2307.36	4.20	25.00	5.60	31.20	3.46	3198
M 14	50	2289.36	4.50	26.00	5.90	32.50	3.10	3220
M 15	50	2271.36	4.60	27.00	6.50	36.00	2.63	3280
M 16	80	2293.04	4.40	25.80	5.80	32.20	3.35	3210
M 17	70	2275.04	4.40	25.90	5.80	32.30	3.19	3214
M 18	60	2257.04	4.50	26.00	5.90	32.50	3.16	3228
M 19	80	2260.72	4.10	24.20	5.40	30.20	3.69	3185
M 20	70	2242.72	4.20	24.70	5.50	30.90	3.58	3193
M 21	70	2228.40	4.10	24.00	5.40	30.00	3.78	3180

B (CS), and C (DS) were tested by the ANOVA method for the concrete features in the two fresh and hardened phases, as shown in Tables 6 to 12. According to the developed models, the F-values obtained for slump, F_S7, C_S7, F_S28, C_S28, Δm/A, and ultrasonic pulse velocity (V) were 9.35, 20.35, 25.02, 18.32, 20.10, 21.58, and 22.84, respectively. These high F-values indicate that the proposed models are statistically significant, with only a 0.01% probability that such values could result from random noise. In ANOVA, model terms are considered statistically significant when the p-value is lower than 0.05, whereas terms with p-values higher than 0.1 are regarded as non-significant [76, 77].

The presence of several non-significant model terms (except those required to maintain model hierarchy) can be reduced by applying model simplification techniques, as suggested by ROUT *et al.* [78]. Overall, the comparison between the predicted R^2 and adjusted R^2 values highlights different levels of model adequacy

Table 5: ANOVA-derived statistical factors.

STATISTICAL FACTOR	FORMULA	DESCRIPTION
Squared sum (SS_f)	$SS_f = \frac{N}{N_{n_f}} \sum_{i=1}^{N_{nf}} (\bar{y}_i - \bar{y})^2$	In order to get a ballpark figure for the standard deviation squared. $\bar{y}$: Mean response; $\bar{y}_i$: Mean of the data collected for each f-factor of the level i; N: Experiments total number; N_{n_f}: Levels number of each f-factor.
Squared mean (MS_i)	$MS_i = \frac{SS_i}{dl_i}$	To get it, divide SS_i by dl_i.
F-Value	$F_i = \frac{MS_i}{MS_e}$	Applied to ensure the statistical model is compatible by comparing computed F-Values to tabulated F-Scores, which must be larger. Average sum of squared errors is known as MS_e.
Contribution (Cont.%)	$Cont.\% = \frac{SS_f}{SS_T} \times 100$	Percent degree influence on response is shown by the variables' contribution (SS_f) to the total variance (SS_T).
Determination coefficient (R^2)	$R^2 = \frac{\Sigma(y_i - \bar{y})^2}{\Sigma(\bar{y}_i - \bar{y})^2}$	When comparing the overall variance to the ratio of explained variation, we can see how well the models match.

Table 6: ANOVA of slump values (mm).

SOURCE	SS_f	df	MS_i	F-VALUE	p-VALUE	CONT. (%)	SIG.
Model- Slump	1836.77	6	306.13	9.35	0.0003	13.33760304	Yes
Linear Mixture	1166.67	2	583.33	17.81	0.0001	25.41477144	Yes
AB	20.25	1	20.25	0.6185	0.4447	0.882260679	No
AC	218.67	1	218.67	6.68	0.0216	9.527108276	Yes
BC	279.43	1	279.43	8.53	0.0112	12.174326	Yes
ABC	222.49	1	222.49	6.79	0.0207	9.693539673	Yes
Residual	458.47	14	32.75				
Cor Total	2295.24	20					
Standard of deviation		5.72		R^2		0.8003	
Mean		59.52		Adjusted R^2		0.7146	
Coefficient of variation. %		9.61		Predicted R^2		0.3347	
Predicted sum-of-squares residual error	1526.94			Adequate Precision		10.257	

Table 7: ANOVA of 7-day flexural strength values (MPa).

SOURCE	SS_f	df	MS_i	F-VALUE	p-VALUE	CONT. (%)	SIG.
Model- F_S7	3.81	6	0.6357	20.35	< 0.0001	14.95764706	Yes
Linear Mixture	2.63	2	1.31	42.05	< 0.0001	30.82352941	Yes
AB	0.4002	1	0.4002	12.81	0.003	9.416470588	Yes
AC	0.5486	1	0.5486	17.56	0.0009	12.90823529	Yes
BC	0.461	1	0.461	14.75	0.0018	10.84705882	Yes
ABC	0.0152	1	0.0152	0.4878	0.4964	0.357647059	No
Residual	0.4374	14	0.0312				
Cor Total	4.25	20					
Standard of deviation		0.177		R^2		0.8971	
Mean		4.04		Adjusted R^2		0.853	
Coefficient of variation. %		4.37		Predicted R^2		0.6193	
Predicted sum-of-squares residual error		1.62		Adequate Precision		17.872	

Table 8: ANOVA of 7-day compressive strength values (MPa).

SOURCE	SS_f	df	MS_i	F-VALUE	p-VALUE	CONT. (%)	SIG.
Model- C_S7	128.76	6	21.46	25.02	< 0.0001	15.24472544	Yes
Linear Mixture	88.25	2	44.13	51.45	< 0.0001	31.34900902	Yes
AB	10.99	1	10.99	12.81	0.003	7.807061164	Yes
AC	21.44	1	21.44	25	0.0002	15.23051787	Yes
BC	15.49	1	15.49	18.06	0.0008	11.00376501	Yes
ABC	0.5639	1	0.5639	0.6575	0.431	0.40058251	No
Residual	12.01	14	0.8577				
Cor Total	140.77	20					
Standard of deviation		0.9261		R^2		0.9147	
Mean		23.71		Adjusted R^2		0.8781	
Coefficient of variation. %		3.91		Predicted R^2		0.6916	
Predicted sum-of-squares residual error		43.42		Adequate Precision		19.722	

among the investigated responses. For slump, F_S7, F_S28, C_S28, $\Delta m/A$, and V, the predicted R^2 values deviate considerably from their corresponding adjusted R^2 values, with differences greater than 0.2. A significant gap between the predicted R^2 and the adjusted R^2 indicates that, although the model fits the experimental data reasonably well, its predictive performance on new or unseen data is weaker. This situation may indicate a high variability in responses: experimental scatter (e.g., due to aggregate hetero-geneity or measurement uncertainty) can affect predictive reliability. Conversely, for C_S7, the predicted R^2 exhibits good agreement with the adjusted R^2, with a difference below 0.2, indicating satisfactory predictive capability and acceptable model reliability for this response. The adequacy of each developed model was assessed using the adequate precision criterion, which evaluates the signal-to-noise ratio. A value greater than 4 is generally considered desirable, as it indicates that the model provides an adequate signal and can be reliably used to explore the design space. For the slump response, an adequate precision value of 10.257 was obtained, confirming a satisfactory signal and demonstrating the reliability of the model for design space navigation. Likewise, adequate precision values of 17.872, 19.722, 16.666, and 17.440 were achieved for F_S7, C_S7, F_S28, and C_S28, respectively, reflecting strong signal

Table 9: ANOVA of 28-day flexural strength values (MPa).

SOURCE	SS_f	df	MS_i	F-VALUE	p-VALUE	CONT. (%)	SIG.
Model- F_S28	9.50	6	1.58	18.32	< 0.0001	14.75256769	Yes
Linear Mixture	7.61	2	3.8	44.01	< 0.0001	35.48085901	Yes
AB	0.4505	1	0.4505	5.21	0.0385	4.206349206	Yes
AC	1.12	1	1.12	12.93	0.0029	10.45751634	Yes
BC	0.6563	1	0.6563	7.59	0.0155	6.127917834	Yes
ABC	0.0288	1	0.0288	0.3334	0.5728	0.268907563	No
Residual	1.21	14	0.0864				
Cor Total	10.71	20					
Standard of deviation		0.294		R^2		0.887	
Mean		5.41		Adjusted R^2		0.8386	
Coefficient of variation. %		5.43		Predicted R^2		0.587	
Predicted sum-of-squares residual error		4.42		Adequate Precision		16.666	

Table 10: ANOVA of 28-day compressive strength values (MPa).

SOURCE	SS_f	df	MS_i	F-VALUE	p-VALUE	CONT. (%)	SIG.
Model- C_S28	286.97	6	47.83	20.10	< 0.0001	14.93334166	Yes
Linear Mixture	229.53	2	114.77	48.22	< 0.0001	35.83315121	Yes
AB	13.02	1	13.02	5.47	0.0347	4.065066034	Yes
AC	34.4	1	34.4	14.45	0.0019	10.74026663	Yes
BC	19.42	1	19.42	8.16	0.0127	6.063255175	Yes
ABC	0.7918	1	0.7918	0.3327	0.5732	0.247213463	No
Residual	33.32	14	2.38				
Cor Total	320.29	20					
Standard of deviation		1.54		R^2		0.896	
Mean		30.05		Adjusted R^2		0.8514	
Coefficient of variation. %		5.13		Predicted R^2		0.6214	
Predicted sum-of-squares residual error		121.25		Adequate Precision		17.440	

strength and robust model performance. Furthermore, the models developed for the quantity of water absorbed per unit surface ($\Delta m/A$) and ultrasonic pulse velocity (V) exhibited adequate precision values of 17.714 and 18.719, respectively, further confirming that all proposed models possess sufficient signal-to-noise ratios.

Overall, the obtained results confirm the statistical validity of the developed models and their suitability for optimization and design purposes within the studied domain.

The mathematical models established in this study are presented in Equations 5–11, which define the relationships between the investigated factors and their corresponding responses.

$$\text{Slump (mm)} = + 75.50A + 45.74B + 44.55C - 17.36AB + 57.044AC + 64.48BC - 335.65ABC \quad (5)$$

$$\text{7-day } F_S \text{ (MPa)} = + 4A + 3.89B + 2.72C + 2.44AB + 2.86AC + 2.62BC - 2.78ABC \quad (6)$$

$$\text{7-day } C_S \text{ (MPa)} = + 23.54A + 23B + 15.85C + 12.79AB + 17.86AC + 15.18BC - 16.9ABC \quad (7)$$

Table 11: ANOVA results for the quantity of water absorbed per unit surface Δm/A (kg.m^{-2}.h$^{-1/2}$).

SOURCE	SS_f	df	MS_i	F-VALUE	p-VALUE	CONT. (%)	SIG.
Model- Δm/A	17.61	6	2.94	21.58	< 0.0001	15.06147541	Yes
Linear Mixture	14.08	2	7.04	51.76	< 0.0001	36.06557377	Yes
AB	0.5374	1	0.5374	3.95	0.0668	2.75307377	Yes
AC	1.99	1	1.99	14.62	0.0019	10.19467213	Yes
BC	1.1	1	1.1	8.08	0.013	5.635245902	Yes
ABC	0.0059	1	0.0059	0.0432	0.8384	0.03022541	No
Residual	1.9	14	0.136				
Cor Total	19.52	20					
Standard of deviation		0.3688		R^2		0.9024	
Mean		3.8		Adjusted R^2		0.8606	
Coefficient of variation. %		9.71		Predicted R^2		0.6246	
Predicted sum-of-squares residual error		7.33		Adequate Precision		17.714	

Table 12: ANOVA of ultrasonic pulse velocity values V (m/s).

SOURCE	SS_f	df	MS_i	F-VALUE	p-VALUE	CONT. (%)	SIG.
Model- V	91665.52	6	15277.59	22.84	< 0.0001	15.12632673	Yes
Linear Mixture	73288.07	2	36644.03	54.78	< 0.0001	36.28121782	Yes
AB	4315.79	1	4315.79	6.45	0.0236	4.273059406	Yes
AC	11050.04	1	11050.04	16.52	0.0012	10.94063366	Yes
BC	7163.15	1	7163.15	10.71	0.0056	7.092227723	Yes
ABC	446.88	1	446.88	0.6681	0.4274	0.442455446	No
Residual	9364.29	14	668.88				
Cor Total	101000	20					
Standard of deviation		25.86		R^2		0.9073	
Mean		3175.24		Adjusted R^2		0.8676	
Variation coefficient. %		0.8145		Predicted R^2		0.6622	
Predicted sum-of-squares residual error		34129.01		Adequate Precision		18.719	

$$\text{28-day } F_S \text{ (MPa)} = +5.25A + 5.77B + 3.36C + 2.59AB + 4.077AC + 3.125BC - 3.819ABC \quad (8)$$

$$\text{28-day } C_S \text{ (MPa)} = +29.3A + 31.94B + 18.69C + 13.92AB + 22.624AC + 17BC - 20ABC \quad (9)$$

$$\Delta m/A \text{ (kg.m}^{-2}\text{.h}^{-1/2}\text{)} = +3.91A + 3.28B + 6.62C - 2.83AB - 5.44AC - 4.045BC + 1.72ABC \quad (10)$$

$$V \text{ (m/s)} = +3168.15A + 3202.079B + 2969.82C + 253.42AB + 405.51AC + 326.49BC - 475.694ABC \quad (11)$$

Compared with the reference normal distribution, the residuals of slump, F_S7, F_S28, C_S7, C_S28, Δm/A, and V are illustrated in the normal probability plots (Figure 5). In all cases, the residuals are closely aligned with the red diagonal reference line, indicating an approximately normal distribution. This behavior confirms that the errors are random rather than systematic, thereby demonstrating the consistency and robustness of the developed models. Figure 6 shows the relationship between the predicted values and the experimental measurements for the seven studied responses, highlighting the accuracy of the developed models. A strong agreement between predicted and observed data is evident from the tight clustering of points along the black diagonal line, reflecting a high level of correlation. This close correspondence validates the predictive capability of the models. Furthermore, the applied color coding offers additional insight into the influence of the studied variables on the prediction distribution. Overall, these results confirm that the proposed models are accurate and reliable for predicting both fresh and hardened properties of concrete. Figures 7a-g provides a detailed analysis of the effects of RS, CS, and DS on both fresh and hardened concrete properties. The mix designs are shown in the ternary graphs, where the equilateral triangle's vertices have the maximum proportions of RS, CS, and DS, respectively. This helps to illustrate the importance of each component. In order assess the effects of the three parameters under research, these plots show the observed response values for the many optimum concrete combinations. Curves are color-coded to indicate the intensity of the responses resulting from the interaction of the input variables, with blue representing the lowest responses and red indicating the highest. Figure 7a shows that the concretes exhibit a plastic workability class, with slump values ranging from 50 mm to 80 mm. The findings also demonstrate that RS has a pronounced positive effect on the workability of fresh mixes, which is reflected in the elevated slump values for mixes M21 (reference concrete 100% RS), M19 (0.8 RS + 0.2 DS), M16 (0.6 RS + 0.4 DS), and M12 (0.4 RS + 0.6 DS). The concrete made with 100% RS demonstrates better workability than that made with 100% CS (M6), this is because CS granules have an angular form and absorb more water than other materials. While RS grains are smooth, round, and spherical, they allow particles to move more easily in their fresh form, while CS grains are more angular and hence decrease the effective water content in the mixture. For workability, 100% DS (M1) prepared concrete is on par with 100% CS. In terms of workability, the reference concrete outshines the DS-based concrete, due to the high water absorption and fine particle size of DS, which reduce the available water in the mix, increase cohesion, and potentially limit slump. These observations are consistent with the findings reported by DOUARA and GUETTALA [2]. Similar to what SAHRAOUI and BOUZIANI [56] found, Figure 7a demonstrates that the workability of the concretes is improved when the proportion of RS in binary and ternary systems is increased. The binary mixes of 0.8 RS + 0.2 DS and 0.6 RS + 0.4 DS showed the greatest slump value of 80 mm. The slump values for concretes made with ternary sand mixes varied between 50 mm and 70 mm. The mixture including 60% RS, 20% CS and 20% DS produced the highest slump of 70 mm. The workability of the concretes was enhanced up to a content of about 0.4 DS when RS was replaced with DS and by 0.4 CS when DS was substituted for RS. Beyond this level, the workability clearly decreased for both types of sand, which is consistent with the findings of BOUZIANI [50]. Figures 7b and 6c show an increase in 7-day flexural and compressive strengths for mixes M9-M11, and M13-M20. For the 28-day compressive and flexural strengths (Figures 7d and 6e), a significant improvement is observed in mixes M10, M11, M14, M15, M17, M18, and M20. The curves exhibit almost similar trends. It can be observed that the 7-day compressive strength is primarily influenced by the RS content, followed by CS and DS dosages. In contrast, the 28-day compressive strength is mainly controlled by the CS content, followed by RS and DS. The results indicate that increasing the CS proportion leads to higher compressive strength, with an optimum effect observed at approximately 60%. This feature is particularly beneficial from both economic and environmental perspectives.

The maximum 28-day compressive strength of 36 MPa was achieved with the binary combination of 0.4 RS and 0.6 CS, while for the ternary mixture (0.2 RS + 0.6 CS + 0.2 DS), a maximum compressive strength of 34.70 MPa was recorded. Granular impact [14, 15], physico-chemical impact [7], and the limestone fillers' chemical reactions in CS [9] are three complementary mechanisms that improve compactness, which in turn enhances compressive strength. The angular structure, big size, and a significant fine content (5.04%) also contribute. Cement paste and grain particles stick together more firmly because of the limestone content of CS. These results are in line with those of FARRAN *et al*. [13], who proved that the cement paste and limestone grains formed a strong link, and ACHOUR *et al*. [10], who proved that the fine particles of limestone aggregates improve the paste-aggregate adhesion. The improvement in concrete strength observed in the results can be mainly attributed to two key factors related to CS: particle angularity and the limestone filler effect. The synergy between angular particle shape and limestone fines (physical and microstructural effect) explains the superior performance of mixes with optimized CS content. However, an excessive amount of fines or poor grading can negatively affect workability and may offset strength gains. The strength enhancement is not due to a single factor, but rather the combined effect of improved interfacial bonding and matrix densification induced by CS characteristics. A positive role for DS is observed up to an ideal content of around 40% in both binary (CS-DS and RS-DS) and ternary mixes. DS improves compactness by reducing void volume; however, exceeding 40% DS leads to a decrease in compressive strength. This decrease is caused by the increased porosity of DS, which is a result of its small particle size, consistent diameter, rounded shape, and water absorption capability. In line with previous research [1, 2, 50, 56] these results. No matter how old the concrete was, the flexural strengths of mixes made with binary and ternary materials followed patterns comparable to the compressive strengths. With hydration came an increase in compressive strength and,

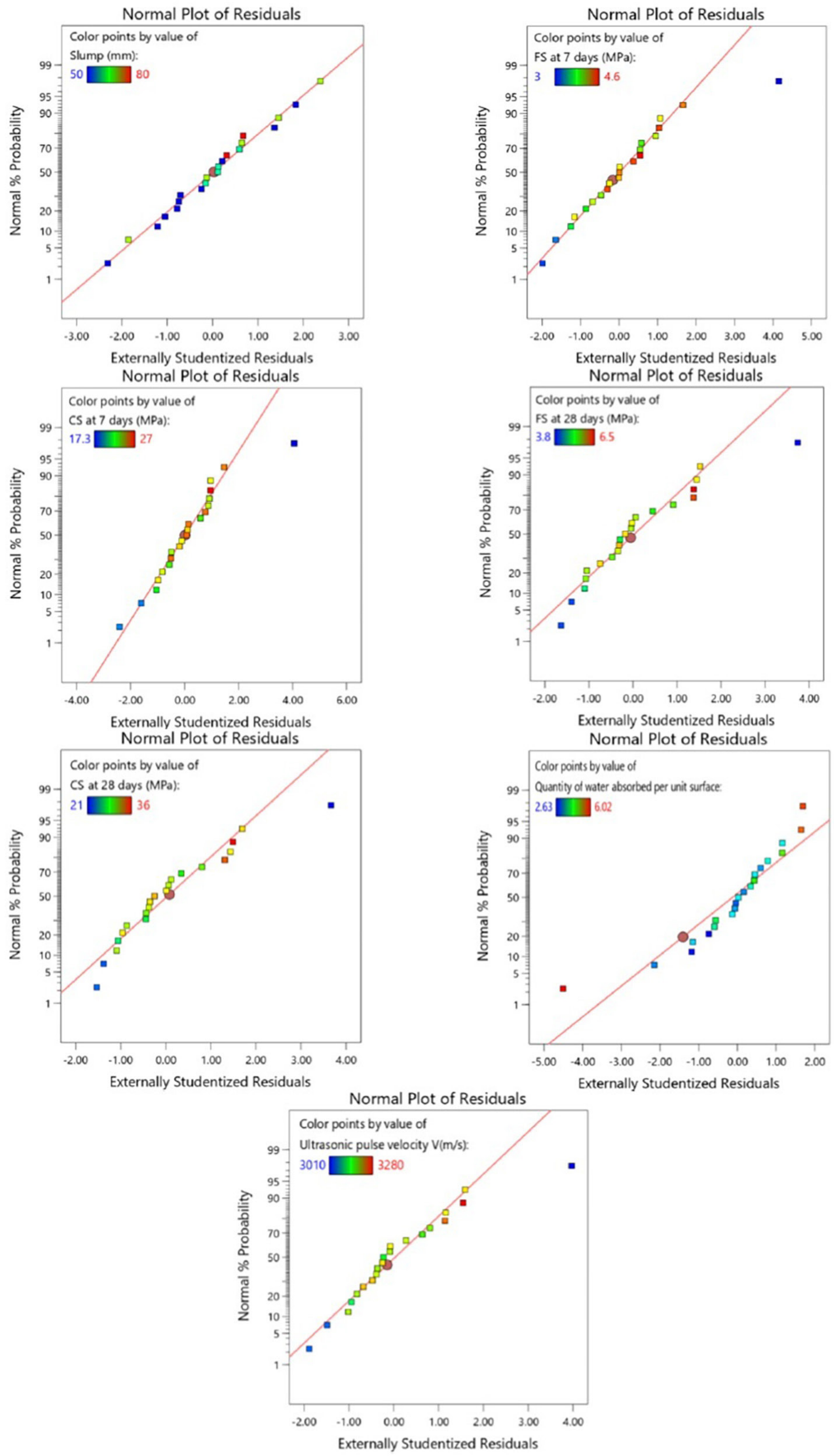

Figure 5: Statistical validation of the developed models: normal residual distributions.

to variable degrees, flexural strength as well. After 28 days, the binary mixture with 0.4 RS and 0.6 CS had a maximum flexural strength of 6.50 MPa, whereas the ternary combination with 20% RS, 60% CS, and 20% DS had a maximum flexural strength of 6.30 MPa. A reduction in the amount of water absorbed (Δm/A) is noted for mixes M4-M6, M9-M11, M13-M15, M17, M18, and M20, as illustrated in Figure 7f. Finally, ultrasonic pulse velocity

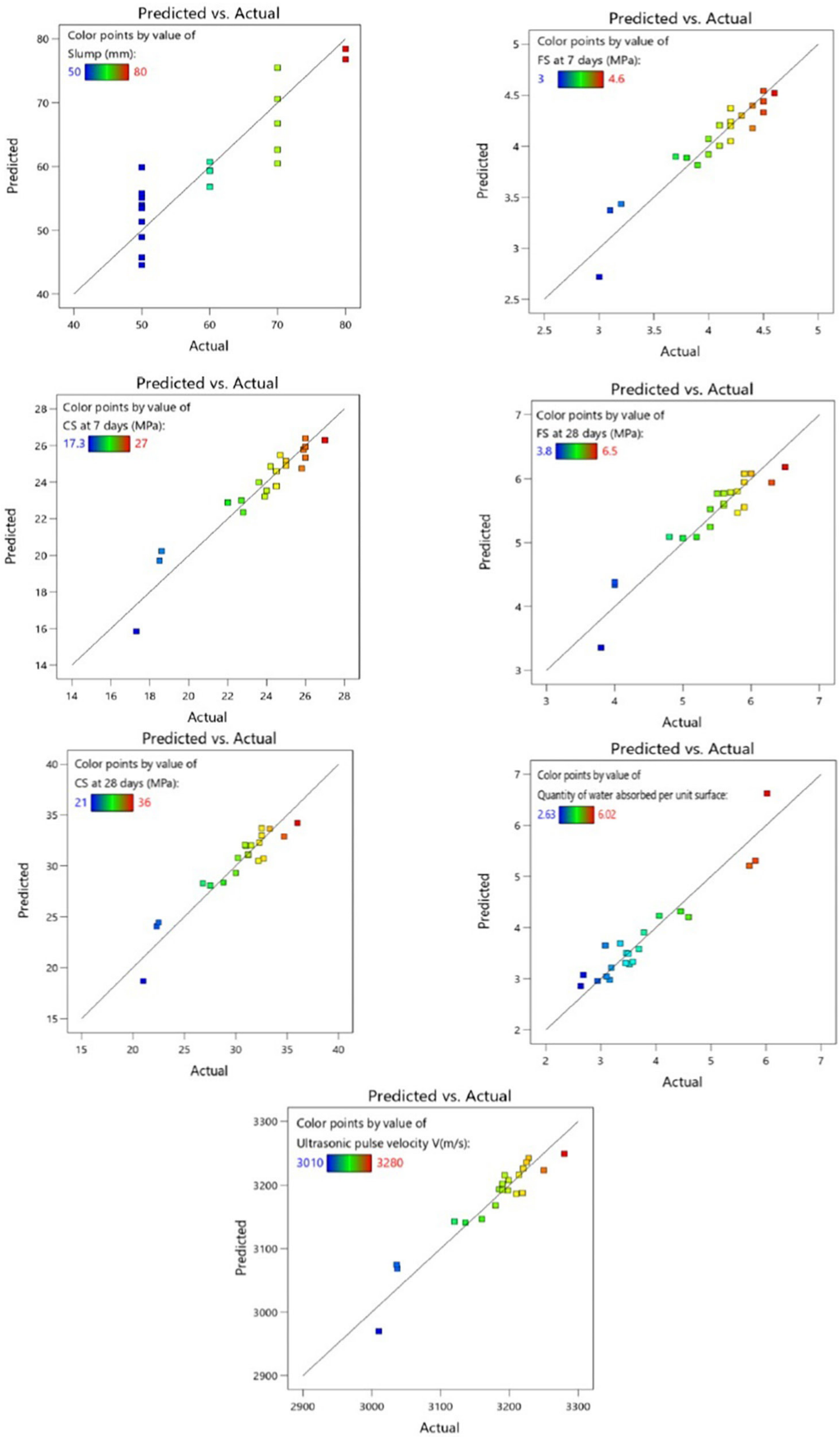

Figure 6: Statistical validation of the developed models: predicted versus measured values of mechanical and physical responses.

(V) is particularly high in mixes M5, M6, M10, M11, M14, M15, M17, M18, and M20, as presented in Figure 7g. Figure 8 clearly illustrates the combined effect of fine aggregate types on compressive strength (C_S) and open porosity (ε). The results show that the binary mixture M15 achieved the highest 28-day compressive strength, while outperforming the reference concrete (M21) by about 20%, and along with the highest dynamic elasticity modulus

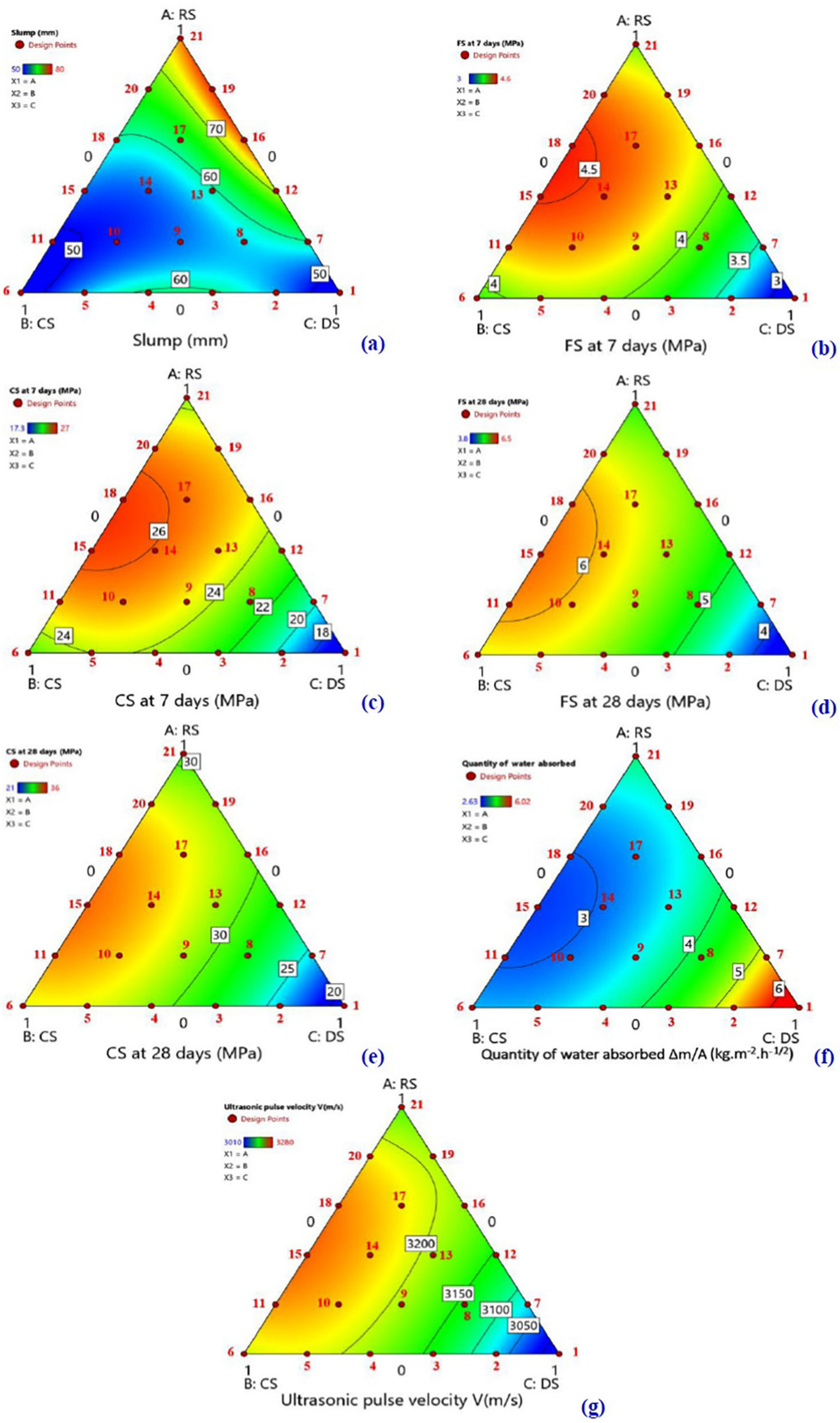

Figure 7: Response surface visualization using ternary contour plots for slump (a), mechanical strengths (b), (c), (d), (e), water absorption (f), and ultrasonic pulse velocity (g).

and the lowest open porosity. M10, a ternary combination, outperformed M21 in terms of 28-day compressive strength, an improvement of about 15.67%. These results can be attributed to the influence of the fine aggregate type, particle size, adherence, and overall material density on compressive strength, dynamic elasticity modulus, and open porosity.

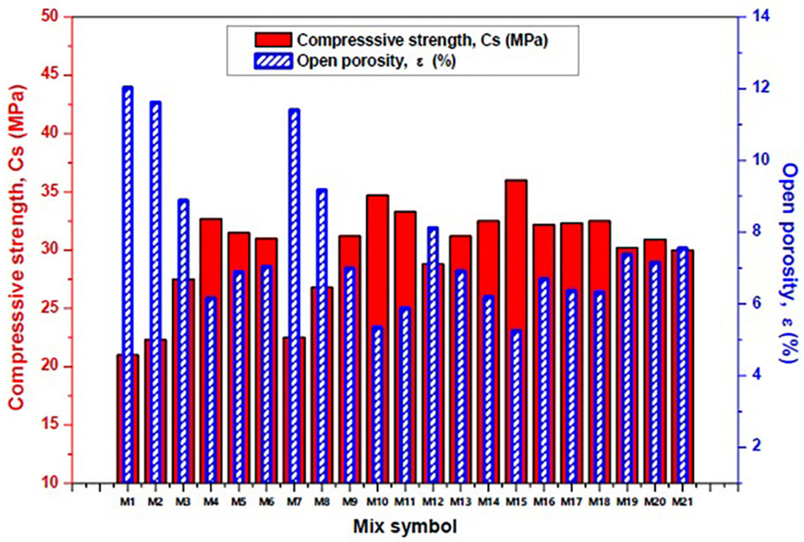

Figure 8: Influence of fine aggregate type-proportion on concrete compressive strength and open porosity.

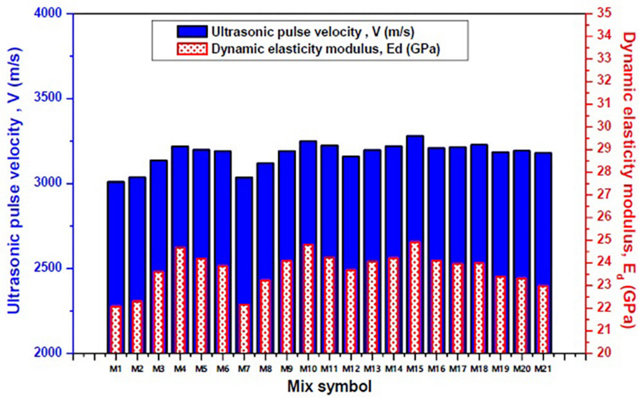

Figure 9: Influence of fine aggregate type-proportion on ultrasonic pulse velocity and dynamic elastic modulus.

Figure 9 depicts the combined effect of fine aggregate types on UPV (V) and dynamic elasticity modulus (E_d). The highest E_d and V values were observed for the binary mixture M15; this is explained by the fact that the E_d depends heavily on the nature, quality, and adherence of the fine aggregates as well as the material density. A reduction in E_d is generally associated with increased porosity, which also affects V. Additionally, the type, size, and adherence of the fine aggregates, together with material density, significantly influence the increase in V of the concrete. Based on the evaluation according to IS 13311-1 [79], the quality of all tested mixtures can be classified as medium-strength concretes.

4. DESIRABILITY-BASED MULTI-OBJECTIVE OPTIMIZATION AND EXPERIMENTAL VALIDATION

Finally, the multi-objective optimization framework adopted in this study incorporated experimental validation and desirability function analysis (DFA). Additional experimental tests were conducted to confirm the reliability of the optimization results obtained through the desirability function. The combination of predictive modeling and experimental validation offers an effective approach for developing concrete mixtures with reduced environmental impact, representing a significant step toward more sustainable construction practices. Moreover, this approach contributes to saving time, cost, and material resources by limiting extensive experimental trials, while promoting environmentally friendly solutions. Accurate prediction of concrete properties also enhances the reliability and durability of building structures. Desirability-based modeling offers fundamentally different insights compared to traditional optimization approaches, particularly in complex systems like concrete mix design, by: transforming a single-objective problem into a multi-criteria decision framework, quantification of trade-offs between properties, identification of a global optimum region, not a single point, integration of performance

Table 13: Criteria and solutions for optimization.

FACTORS	UNIT	DESIG.	THE GOAL	FINDINGS FROM OPTIMIZATION	DESIRABILITY
RS	%	A	Range	0.45873	0.913 (91.3%)
CS	%	B	Range	0.544127	
DS	%	C	Range	0	
Slump	mm	-	Range	55.0019	
F_S at 7 days	MPa	-	Maximize	4.54615	
C_S at 7 days	MPa	-	Maximize	26.4165	
F_S at 28 days	MPa	-	Maximize	6.17571	
C_S at 28 days	MPa	-	Maximize	34.1885	
Δm/A	$kg.m^{-2}.h^{-1/2}$	-	Minimize	2.86487	
V	m/s	-	Maximize	3249.47	

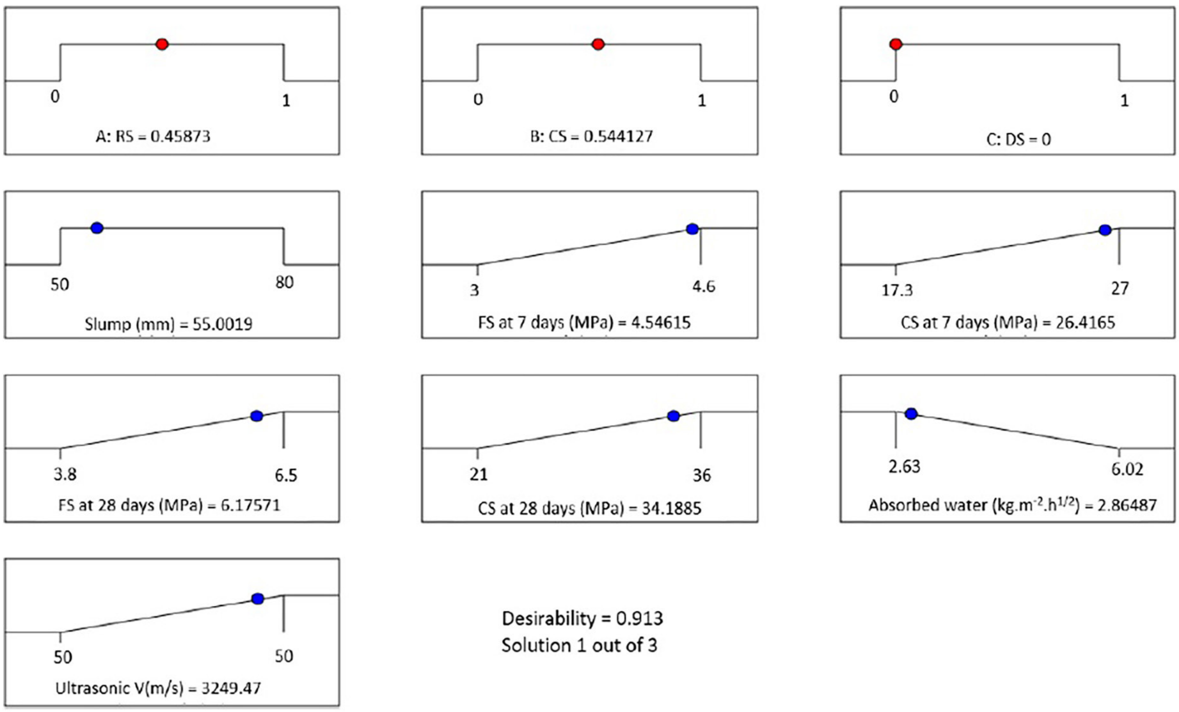

Figure 10: Desirability function-based optimization ramp diagram for the studied responses.

priorities and design criteria, enhanced interpretation of multi-variable interactions, and direct link between modeling and practical validation. The optimization technique took into account several essential response factors to determine the ideal ratios for the combination. AWOLUSI *et al*. [80] assert that when optimizing multiple performance metrics simultaneously, achieving a compromise optimum is more pertinent than focusing on a singular performance indicator. To achieve this objective, it is essential to define appropriate criteria and levels of significance for all pertinent components, including input variables and response parameters. Optimization performance is assessed using a desirability function ranging from 0 to 1, where values closer to 1 indicate more favorable outcomes [81, 82]. Table 13 summarizes the optimization objectives and corresponding desirability functions adopted in this study. The selected mix proportions were 45.873% RS, 54.4127% CS, and 0% DS, ensuring compliance with the experimentally investigated ranges. The evaluated response parameters included slump, flexural strength at 7 and 28 days (F_S7 and F_S28), compressive strength at 7 and 28 days (C_S7 and C_S28), quantity of water absorbed per unit surface area (Δm/A), and ultrasonic pulse velocity (V). The optimization

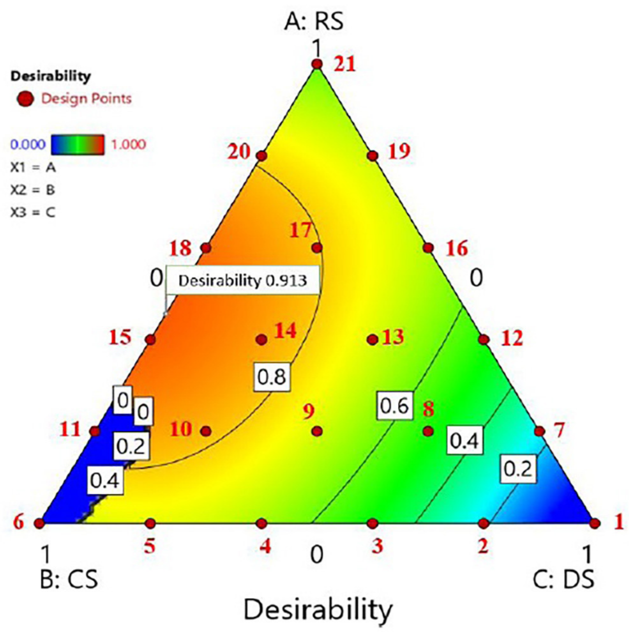

Figure 11: Ternary contour plots of the desirability function.

Table 14: Experimental confirmation of the findings.

FACTORS	UNIT	DESIG.	THE GOAL	MODEL PREDICTION	LABORATORY EXPERIMENT	ABSOLUTE ERROR (%)	DESIRABILITY
RS	%	A	Range	0.45873	0.45873	-	0.913 (91.3%)
CS	%	B	Range	0.544127	0.544127	-	
DS	%	C	Range	0	0	-	
Slump	mm	-	Range	55.0019	60	8.33	
F_s at 7 days	MPa	-	Maximize	4.54615	4.222	7.67	
C_s at 7 days	MPa	-	Maximize	26.4165	26.129	1.1	
F_s at 28 days	MPa	-	Maximize	6.17571	6.785	8.98	
C_s at 28 days	MPa	-	Maximize	34.1885	33.552	1.89	
Δm/A	$kg.m^{-2}.h^{-1/2}$	-	Minimize	2.86487	2.725	5.13	
V	m/s	-	Maximize	3249.47	3245	0.14	

criteria were defined to maximize flexural and compressive strengths at both curing ages (MPa), maximize V (m/s), minimize Δm/A ($kg.m^{-2}.h^{-1/2}$), and achieve a target average slump value.

Figure 10 illustrates the optimization results in the form of ramp plots, whereas Figure 11 depicts the ternary response surfaces and the corresponding desirability contours. The final stage of the mix design methodology consisted of experimental validation, in which concrete specimens were prepared using the optimal variable proportions obtained from the optimization process. These specimens were subsequently tested to assess the corresponding responses. The experimental results, together with the predicted optimal values, are reported in Table 13. The experimental error between the predicted and measured results was calculated using Equation 12, and the corresponding values are summarized in Table 14. The experimental error for all responses was found to be less than 9%, confirming the reliability and accuracy of the developed response models and the effectiveness of the optimization procedure.

$$\text{Absolute experimental error}(\%) = \left(1 - \frac{\text{Predicted value}}{\text{Experimental value}}\right) \times 100 \quad (12)$$

5. CORRELATIONS

5.1. Correlation among compressive strength, open porosity, and density

Figure 12 shows the correlation among compressive strength Cs (MPa), open porosity ε (%), and density ρ (kg/m^3). The results reveal that Cs decreases with increasing ε, and ρ. Moreover, modeling compressive strength depending on these parameters allows it to be expressed by a linear relationship, as given in Equation 13.

$$Cs\ (MPa) = (25 / (w/c)) - (4.5 / (w/c)) \times \varepsilon\ (\%) \times \rho\ (kg/m^3) \times 10^{-3} / g\ (m/s^2) \quad (13)$$

Coefficient of regression (**R^2 = 0.995**)

$$Cs\ (MPa) = (25 / 0.56) - (4.5 / 0.56) \times \varepsilon\ (\%) \times \rho\ (kg/m^3) \times 10^{-3} / 9.81$$

A very strong linear relationship was observed. Table 15 presents a comparison between the experimental and predicted values of the 28-day compressive strength depending on open porosity ε (%), and density ρ (kg/m^3). The relative error (%) calculated for the different experimental data points generally remains below 4%, allowing the conclusion that the 28-day compressive strength can be reliably estimated solely from the determination of open porosity, and density.

5.2. Correlation among compressive strength and the ultrasonic pulse velocity

Figure 13 illustrates the correlation among compressive strength Cs (MPa) and the UPV V (m/s) of concretes. The results indicate that Cs increases with increasing UPV. Furthermore, modeling compressive strength depending on the UPV allows the 28-day compressive strength to be expressed by an exponential relationship, as given by:

$$C_S\ (MPa) = 0.038 \times \exp(0.0021 \times v\ (m/s)); \text{ Coefficient of regression } (\mathbf{R^2 = 0.997}) \quad (14)$$

The advanced correlation generally corroborates the findings of DEMIRBOĞA *et al*. [83]. Table 15 presents a comparison between the experimental and predicted values of the 28-day compressive strength depending on the upv. There is typically less than a 4% relative error when calculating the various experimental data points, which allows the conclusion that the 28-day compressive strength can be reliably estimated solely by measuring the ultrasonic pulse velocity of concrete.

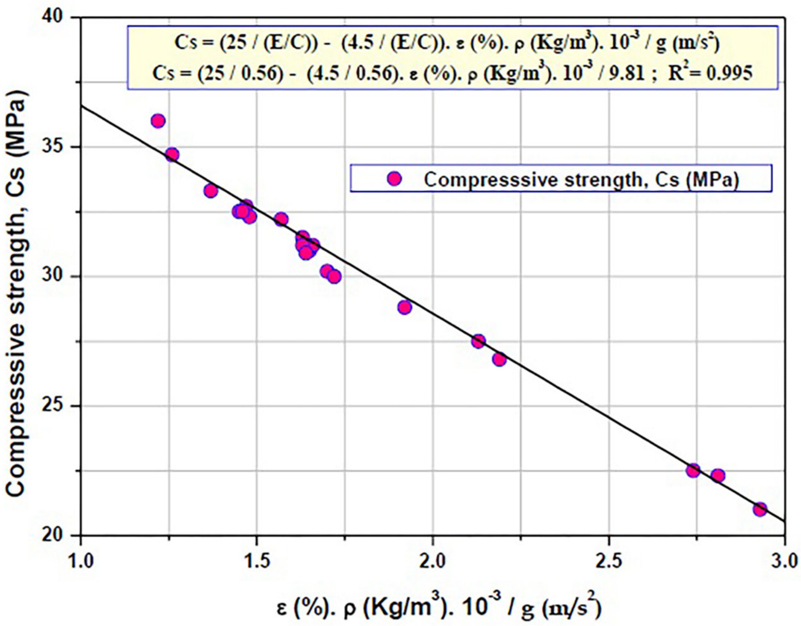

Figure 12: Relationship between compressive strength, open porosity, and density.

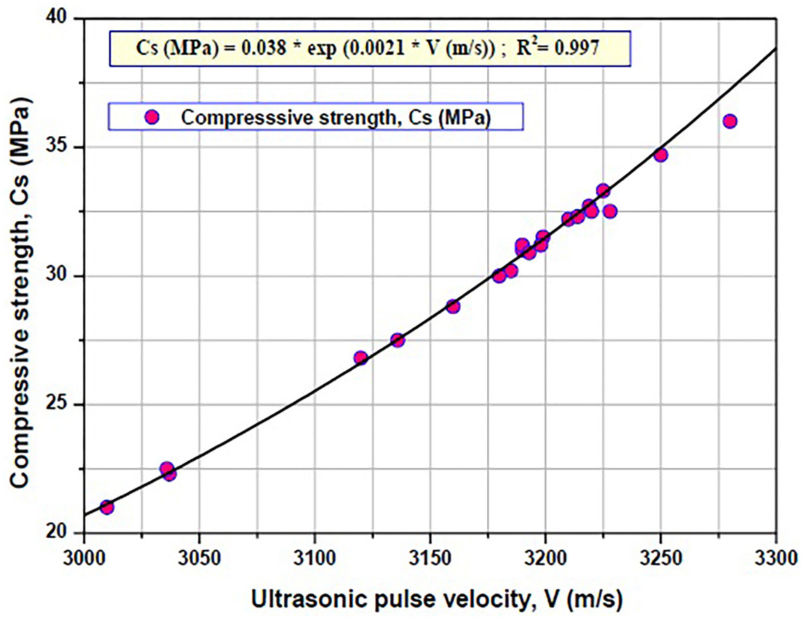

Figure 13: Relationship between compressive strength and ultrasonic pulse velocity.

Table 15: Estimated and experimental 28-day compressive strength values.

MIX	Cs (MPa) AS A FUNCTION ON ε (%) AND ρ (kg/m³)			Cs (MPa) AS A FUNCTION ON V (m/s)		
	Cs MEASURED	Cs ESTIMATED	RELATIVE ERROR (%)	Cs MEASURED	Cs ESTIMATED	RELATIVE ERROR (%)
M 1	21.00	21.07	0.30	21.00	21.13	0.63
M 2	22.30	22.08	1.00	22.30	22.37	0.29
M 3	27.50	27.50	0.00	27.50	27.53	0.12
M 4	32.70	32.84	0.40	32.70	32.78	0.24
M 5	31.50	31.55	0.20	31.50	31.43	0.23
M 6	31.00	31.36	1.20	31.00	30.84	0.51
M 7	22.50	22.61	0.50	22.50	22.32	0.81
M 8	26.80	27.05	0.90	26.80	26.62	0.65
M 9	31.20	31.33	0.40	31.20	30.84	1.15
M 10	34.70	34.55	0.40	34.70	34.98	0.81
M 11	33.30	33.64	1.00	33.30	33.19	0.32
M 12	28.80	29.17	1.30	28.80	28.96	0.55
M 13	31.20	31.57	1.20	31.20	31.36	0.52
M 14	32.50	33.02	1.60	32.50	32.85	1.06
M 15	36.00	34.87	3.10	36.00	37.26	3.49
M 16	32.20	32.05	0.50	32.20	32.16	0.11
M 17	32.30	32.77	1.50	32.30	32.43	0.42
M 18	32.50	32.95	1.40	32.50	33.40	2.78
M 19	30.20	30.96	2.50	30.20	30.52	1.05
M 20	30.90	31.50	1.90	30.90	31.04	0.44
M 21	30.00	30.83	2.80	30.00	30.20	0.67

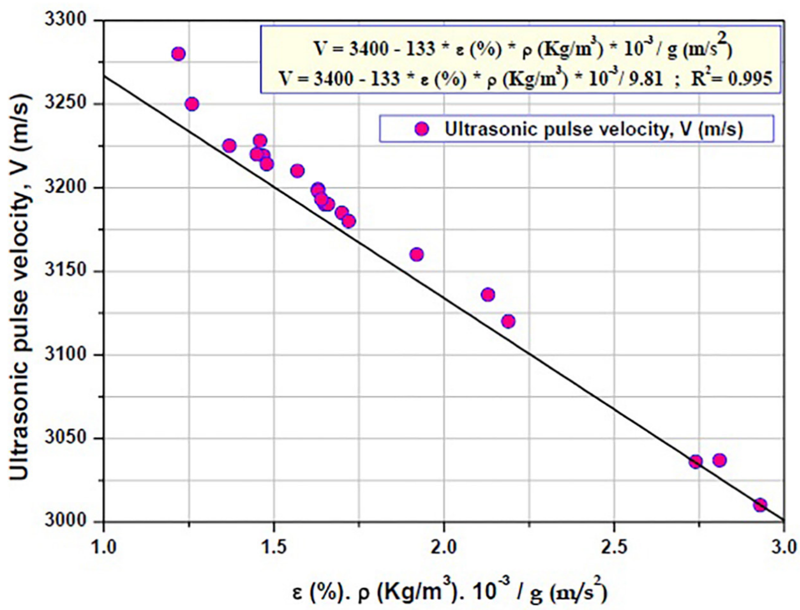

Figure 14: Relationship between ultrasonic pulse velocity, open porosity, and density.

5.3. Correlation among ultrasonic pulse velocity, open porosity, and density

Figure 14 illustrates the correlation among ultrasonic pulse velocity V (m/s), open porosity ε (%), and density ρ (kg/m³). It can be observed that V decreases with increasing ε, and ρ. The modeling the UPV depending on the open porosity, and density allows it to be expressed as a linear relationship, as follows:

$$V\ (m/s) = 3400 - 133 \times \varepsilon\ (\%) \times \rho\ (Kg/m^3) \times 10^{-3} / g\ (m/s^2) \quad (15)$$

Coefficient of regression (R^2 = **0.995**).

This finding is consistent with OMRANE and RABEHI [84]. A strong linear relationship was observed between ultrasonic pulse velocity, open porosity, and density. Table 16 provides a comparison between the experimental and predicted values of UPV depending on the open porosity and density. The relative errors (%) for the various experimental points are generally below 2%, indicating that ultrasonic pulse velocity can be reliably estimated solely from measurements of open porosity and density.

5.4. Correlation among dynamic elasticity modulus, open porosity, and density

Figure 15 illustrates the correlation among dynamic elasticity modulus E_d (GPa), open porosity ε (%), and density ρ (kg/m³). The results indicate that the E_d decreases with increasing ε and ρ. Furthermore, modeling the E_d depending on these parameters allows it to be represented by an exponential relationship, as expressed in Equation 16.

$$E_d\ (GPa) = 8.35 \times \exp(-0.62 \times \varepsilon\ (\%) \times \rho\ (kg/m^3) \times 10^{-3} / g\ (m/s^2)) + 20.82 \quad (16)$$

Coefficient of regression (**R^2 = 0.916**)

A strong exponential relationship was observed between the dynamic elasticity modulus E_d (GPa), open porosity ε (%), and density ρ (kg/m³). Table 16 presents a comparison between the experimental and predicted values of the E_d depending on the ε and ρ. The relative errors (%) for the various experimental points are generally below 4%, indicating that the dynamic elasticity modulus can be reliably estimated solely from measurements of open porosity and density. According to OMRANE and RABEHI [84], this outcome is in line with what was found.

Table 16: Estimated and experimental ultrasonic pulse velocity and dynamic modulus of elasticity values.

MIX	V (m/s) A FUNCTION ON ε (%) AND ρ (kg/m³)			E_D (GPa) A FUNCTION ON ε (%) AND ρ (kg/m³)		
	V MEASURED	V ESTIMATED	RELATIVE ERROR (%)	E_d MEASURED	E_d ESTIMATED	RELATIVE ERROR (%)
M 1	3010.00	3009.79	0.01	22.07	22.17	0.46
M 2	3037.00	3026.54	0.34	22.29	22.28	0.04
M 3	3136.00	3116.25	0.63	23.60	23.04	2.35
M 4	3219.00	3204.60	0.45	24.67	24.18	2.01
M 5	3199.00	3183.29	0.49	24.18	23.86	1.33
M 6	3190.00	3180.22	0.31	23.86	23.82	0.17
M 7	3036.00	3035.37	0.02	22.15	22.35	0.87
M 8	3120.00	3108.75	0.36	23.22	22.97	1.07
M 9	3190.00	3179.70	0.32	24.08	23.81	1.13
M 10	3250.00	3232.89	0.53	24.80	24.65	0.61
M 11	3225.00	3217.88	0.22	24.23	24.39	0.66
M 12	3160.00	3143.99	0.51	23.67	23.35	1.34
M 13	3198.00	3183.60	0.45	24.05	23.86	0.79
M 14	3220.00	3207.57	0.39	24.20	24.22	0.12
M 15	3280.00	3238.33	1.27	24.91	24.75	0.64
M 16	3210.00	3191.57	0.57	24.09	23.98	0.44
M 17	3214.00	3203.49	0.33	23.96	24.16	0.86
M 18	3228.00	3206.40	0.67	23.97	24.21	0.97
M 19	3185.00	3173.54	0.36	23.38	23.73	1.49
M 20	3193.00	3182.44	0.33	23.31	23.85	2.32
M 21	3180.00	3171.46	0.27	22.97	23.70	3.16

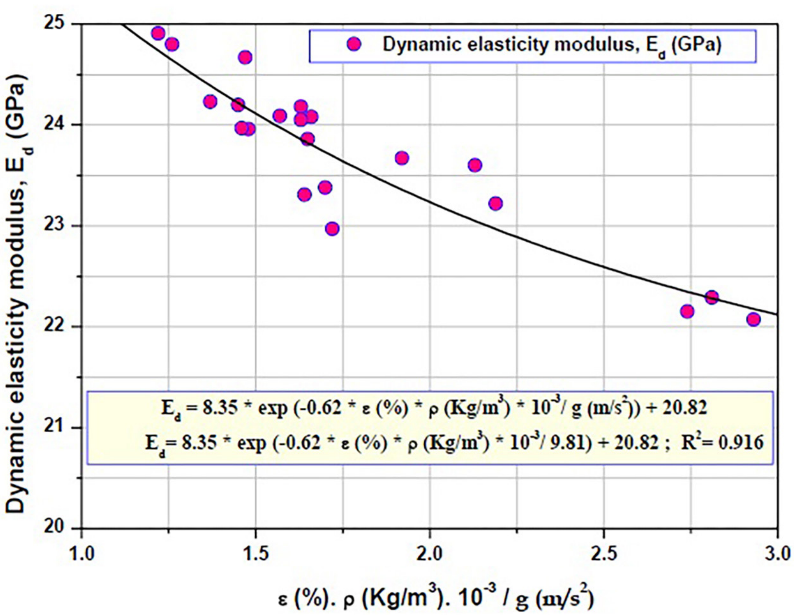

Figure 15: Relationship between dynamic elastic modulus, open porosity, and density.

6. CONCLUSIONS

Based on the results of this study, the following conclusions could be drawn:

1. RS significantly improves the slump due to its spherical particle shape and smooth surface, while CS and DS reduce workability because of angularity and high water absorption. The optimal workability was achieved at 40% DS or CS substitution levels.
2. CS enhances both compressive and flexural strengths due to its angular structure and limestone composition, which improve paste-aggregate adhesion and compactness. The best 28-day compressive strength (36 MPa) was recorded for the mix consisting of 0.4 RS + 0.6 CS.
3. With a rise of approximately 15.67% compared to the reference concrete (M21), mixture M10 had the greatest 28-day compressive strength among the ternary mixes.
4. Increasing CS and moderate DS content reduced open porosity and water absorption. Excess DS (> 40%) increased porosity and decreased strength.
5. Optimal blend obtained via desirability analysis was 45.87% RS, 54.41% CS, and 0% DS, ensuring a balance between workability, flexural and compressive strengths, and water absorbed amount per unit surface after 1 hour, and ultrasonic pulse velocity (UPV). Experimental validation showed prediction errors below 9%, confirming models reliability.
6. As hydration progressed, the concretes exhibited increases in compressive strength and dynamic elasticity modulus, which were accompanied by enhanced flexural strength and reduced open porosity.
7. Strong relationships were established between compressive strength, open porosity, density, UPV, and dynamic elasticity modulus of concretes with different types of fine aggregate ($R^2 > 0.91$), enabling non-destructive property estimation.
8. In addition to their promising physico-mechanical performance, the concretes highlight the feasibility of replacing natural river sand with locally sourced materials, offering economic, technological, and environmental benefits.

7. DATA AVAILABILITY

The data used to support the findings of this study are available from the corresponding author upon request.

8. BIBLIOGRAPHY

[1] NÉCIRA, B., GUETTALA, A., GUETTALA, S., "Study of the combined effect of different types of sand on the characteristics of high performance self-compacting concrete", *Journal of Adhesion Science and Technology*, v. 31, n. 17, pp. 1912–1928, 2017. doi: https://doi.org/10.1080/01694243.2017.1289829.

[2] DOUARA, T.-H., GUETTALA, S., "Effects of curing regimes on the physico-mechanical properties of self-compacting concrete made with ternary sands", *Construction & Building Materials*, v. 195, pp. 41–51, 2019. doi: https://doi.org/10.1016/j.conbuildmat.2018.11.043.

[3] HELIS, L., DOUARA, T.H., OMRANE, M., *et al*., "Synergistic effects of steam curing and recycled concrete powder on the mechanical performance of eco-concrete made with recycled concrete aggregates", *Matéria*, v. 30, e20250332, 2025.

[4] AL MAZROA, A., ALOTAIBI, F.A., RAMAMURTHY, C., *et al*., "Predictive modeling of cementitious green hybrid concrete strength for low-volume roads using RSM", *Matéria*, v. 30, e20240603, 2025.

[5] KUMAR, A.G., RAMASAMY, S., SOUNDARARAJAN, E.K., *et al*., "Sustainable utilization of cement kiln dust and GGBS in the development of eco-friendly concrete composite", *Matéria*, v. 29, e20240054, 2024.

[6] NACHIMUTHU, B., VISWANATHAN, R., SUBRAMANIYAN, Y., *et al*., "Mechanical properties of recycled concrete aggregates with superplasticizer", *Matéria*, v. 29, e20230382, 2024.

[7] CARE, S., LINDER, R., BAROGHEL BOUNY, V., *et al*., *Effect of mineral additions on the concrete use properties: experience plan and static analysis*, Paris, LCPC, 2002.

[8] DETWILER, R.J., TENNIS, P., *The use of limestone in Portland cement: a state of the art review, RP 118*, Skokie, Portland Cement Association, 1996.

[9] CYR, M., LAWRENCE, P., RINGOT, E., "Efficiency of mineral admixtures in mortars, quantification of physical and chemical effects of fine admixtures in relation with compressive strength", *Cement and Concrete Research*, v. 36, n. 2, pp. 264–277, 2006. doi: https://doi.org/10.1016/j.cemconres.2005.07.001.

[10] ACHOUR, T., LECOMTE, A., BEN OUEZDOU, M., *et al*., "Contribution of the fillers limestones to the paste-aggregate bond: Tunisian examples", *Materials and Structures*, v. 41, n. 5, pp. 815–830, 2008. doi: https://doi.org/10.1617/s11527-007-9287-0.

[11] LIAO, K.Y., CHANG, P.K., PENG, Y.N., *et al*., "A study on characteristics of interfacial transition zone in concrete", *Cement and Concrete Research*, v. 34, n. 6, pp. 977–989, 2004. doi: https://doi.org/10.1016/j.cemconres.2003.11.019.

[12] GAO, J.M., QIAN, C.X., LIU, H.F., *et al*., "ITZ microstructure of concrete containing GGBS", *Cement and Concrete Research*, v. 35, n. 7, pp. 1299–1304, 2005. doi: https://doi.org/10.1016/j.cemconres.2004.06.042.

[13] FARRAN, J., JAVELAS, R., MASO, J.C., *et al*., "Study of the existing transition aureole between the aggregates of a mortar and the mass of paste cement hydrated", In: *Colloque International, Liaison de Contact dans les Matériaux Composites Utilisés en Génie Civil*, v. I, Toulouse, pp. 60–76, 1972.

[14] DE LARRARD, F., BELLOC, A., *L'influence du granulat sur la résistance a la compression des bétons*, Bulletin de Liaison des Laboratoires des Ponts et Chaussées, n. 219, Paris, Janvier-Fevrier, pp. 41–52, 1999.

[15] LECOMTE, A., DE LARRARD, F., MECHLING, J.M., "Compressive strength of hydraulic concretes to the unoptimised granular skeleton", *Bulletin LPC*, v. 234, pp. 89–105, 2001.

[16] MENADI, B., KENAI, S., KHATIB, J., *et al*., "Strength and durability of concrete incorporating crushed limestone sand", *Construction & Building Materials*, v. 23, n. 2, pp. 625–633, 2009. doi: https://doi.org/10.1016/j.conbuildmat.2008.02.005.

[17] CELIK, T., MARAR, K., "Effects of crushed stone dust on some properties of concrete", *Cement and Concrete Research*, v. 26, n. 7, pp. 1121–1130, 1996. doi: https://doi.org/10.1016/0008-8846(96)00078-6.

[18] DEHWAH, H.A.F., "Mechanical properties of self-compacting concrete incorporating quarry dust powder, silica fume or fly ash", *Construction & Building Materials*, v. 26, n. 1, pp. 547–551, 2012. doi: https://doi.org/10.1016/j.conbuildmat.2011.06.056.

[19] ZAIN, M.E.M., SAFIUDDIN, M., YOUSUF, K.M., "A study on the properties of freshly mixed high performance concrete", *Cement and Concrete Research*, v. 29, n. 9, pp. 1427–1432, 1999. doi: https://doi.org/10.1016/S0008-8846(99)00108-8.

[20] LOHANI, T.K., PADHI, M., JENA, S., "Optimum utilization of quarry dust as partial replacement of sand in concrete", *International Journal of Applied Sciences and Engineering Research*, v. 1, pp. 391–404, 2012.

[21] AKROUT, K., MOUNANGA, P., LTIFI, M., *et al*., "Rheological, mechanical and structural performances of crushed limestone sand concrete", *International Journal of Concrete Structures and Materials*, v. 4, n. 2, pp. 97–104, 2010. doi: https://doi.org/10.4334/IJCSM.2010.4.2.97.

[22] RAO, K.B., DESAI, V.B., MOHAN, D.J., "Experimental investigation on mode II fracture of concrete with crushed granite stone fine aggregate replacing sand", *Materials Research*, v. 15, n. 1, pp. 41–50, 2011. doi: https://doi.org/10.1590/S1516-14392011005000093.

[23] REDDY, M.V., SATYANARAYANA REDDY, C.N.V., "An experimental study of rock flour and insulator ceramic scrap in concrete", *Journal of the Institution of Engineers (India)*, v. 88, pp. 47–50, 2007.

[24] ILANGOVANA, R., MAHENDRANA, N., NAGAMANIB, K., "Strength and durability properties of concrete containing quarry rock dust as fine aggregates", *ARPN: Journal of Engineering and Applied Sciences*, v. 3, pp. 20–26, 2008.

[25] HAMEED, M.S., SEKAR, A.S.S., "Properties of green concrete containing quarry rock dust and Marble sludge powder as fine aggregates", *ARPN: Journal of Engineering and Applied Sciences*, v. 4, pp. 83–89, 2009.

[26] POON, C.S., SHUI, Z.H., LAM, L., *et al*., "Influence of moisture states of natural and recycled aggregates on the slump and compressive strength of concrete", *Cement and Concrete Research*, v. 34, n. 1, pp. 31–36, 2004. doi: https://doi.org/10.1016/S0008-8846(03)00186-8.

[27] AL-HARTHY, A.S., HALIM, M.A., TAHA, R., *et al*., "The properties of concrete made with fine dune sand", *Construction & Building Materials*, v. 21, n. 8, pp. 1803–1808, 2007. doi: https://doi.org/10.1016/j.conbuildmat.2006.05.053.

[28] BEDERINA, M., MARMORET, L., MEZREB, K., *et al*., "Effect of the addition of wood shavings on thermal conductivity of sand concretes: experimental study and modelling", *Construction & Building Materials*, v. 21, n. 3, pp. 662–668, 2007. doi: https://doi.org/10.1016/j.conbuildmat.2005.12.008.

[29] BEDERINA, M., LAIDOUDI, B., GOULLIEUX, A., *et al*., "Effect of the treatment of wood shavings on the physico-mechanical characteristics of wood sand concretes", *Construction & Building Materials*, v. 23, n. 3, pp. 1311–1315, 2009. doi: https://doi.org/10.1016/j.conbuildmat.2008.07.029.

[30] GUETTALA, S., MEZGHICHE, B., "Compressive strength and hydration with age of cement pastes containing dune sand powder", *Construction & Building Materials*, v. 25, n. 3, pp. 1263–1269, 2011. doi: https://doi.org/10.1016/j.conbuildmat.2010.09.026.

[31] ZEGHICHI, L., BENGHAZI, Z., BAALI, L., "Comparative study of self-compacting concrete with manufactured and dune sand", *Journal of Civil Engineering and Architecture*, v. 6, pp. 1429–1434, 2012.

[32] BELFERRAG, A., KRIKER, A., KHENFER, M.E., "Improvement of the compressive strength of mortar in the arid climates by valorization of dune sand and pneumatic waste metal fibers", *Construction & Building Materials*, v. 40, pp. 847–853, 2013. doi: https://doi.org/10.1016/j.conbuildmat.2012.11.079.

[33] YUSUF, A.Y., OLAWUMI, B.A., "Comparative study on strength properties of concrete made with river sand and dune sand as fine aggregate", *IOSR Journal of Mechanical and Civil Engineering*, v. 12, pp. 71–75, 2015.

[34] ALHOZAIMY, A., JAAFAR, M.S., AL-NEGHEIMISH, A., *et al.*, "Properties of high strength concrete using white and dune sands under normal and autoclaved curing", *Construction & Building Materials*, v. 27, n. 1, pp. 218–222, 2012. doi: https://doi.org/10.1016/j.conbuildmat.2011.07.057.

[35] ALHOZAIMY, A., AL-NEGHEIMISH, A., ALAWAD, O.A., *et al.*, "Binary and ternary effects of ground dune sand and blast furnace slag on the compressive strength of mortar", *Cement and Concrete Composites*, v. 34, n. 6, pp. 734–738, 2012. doi: https://doi.org/10.1016/j.cemconcomp.2012.03.002.

[36] ALHOZAIMY, A., ALAWAD, O.A., JAAFAR, M.S., *et al.*, "Use of fine ground dune sand as a supplementary cementing material", *Journal of Civil Engineering and Management*, v. 20, n. 1, pp. 32–37, 2014. doi: https://doi.org/10.3846/13923730.2013.768541.

[37] ZAITRI, R., BEDERINA, M., BOUZIANI, T., *et al.*, "Development of high performances concrete based on the addition of grinded dune sand and limestone rock using the mixture design modeling approach", *Construction & Building Materials*, v. 60, pp. 8–16, 2014. doi: https://doi.org/10.1016/j.conbuildmat.2014.02.062.

[38] ZAITRI, R., GUETTALA, S., BEDERINA, M., "Physico-mechanical properties of mortars based on the addition of dune sand powder and the recycled fines using the mixture design modeling approach", *Journal of Adhesion Science and Technology*, v. 32, n. 15, pp. 1613–1628, 2018. doi: https://doi.org/10.1080/01694243.2018.1434032.

[39] GHRIEB, A., MITICHE-KETTAB, R., BALI, A., "Stabilization and utilization of dune sand in road engineering", *Arabian Journal for Science and Engineering*, v. 39, n. 3, pp. 1517–1529, 2014. doi: https://doi.org/10.1007/s13369-013-0721-z.

[40] EL-SAYED, M.I., "Sedimentological characteristics and morphology of the aeolian sand dunes in the eastern part of the UAE: a case study from Ar Rub' El Khali", *Sedimentary Geology*, v. 123, n. 3-4, pp. 219–238, 1999. doi: https://doi.org/10.1016/S0037-0738(98)00116-X.

[41] LEE, E., PARK, S., KIM, Y., "Drying shrinkage cracking of concrete using dune sand and crushed sand", *Construction & Building Materials*, v. 126, pp. 517–526, 2016. doi: https://doi.org/10.1016/j.conbuildmat.2016.08.141.

[42] LUO, F.J., HE, L., PAN, Z., *et al.*, "Effect of very fine particles on workability and strength of concrete made with dune sand", *Construction & Building Materials*, v. 47, pp. 131–137, 2013. doi: https://doi.org/10.1016/j.conbuildmat.2013.05.005.

[43] BEDERINA, M., KHENFER, M.E., DHEILLY, R.M., *et al.*, "Reuse of local sand: effect of limestone filler proportion on the rheological and mechanical properties of different sand concretes", *Cement and Concrete Research*, v. 35, n. 6, pp. 1172–1179, 2005. doi: https://doi.org/10.1016/j.cemconres.2004.07.006.

[44] RMILI, A., BEN OUEZDOU, M., "Valorization of the crushed sand and of the desert sand in the composition of the self-compacting concrete", *MATEC Web of Conferences*, v. 2, pp. 01001, 2012.

[45] AZZOUZ, L., BENABED, B., KADRI, E.H., *et al.*, "Effect of sand type on fresh and hardened properties of self-compacting concrete", In: *Proceedings of the2nd International Sustainable Buildings Symposium (ISBS)*, pp. 37–41, Ankara, Turkiye, 2015.

[46] BROUWERS, H.J.H., RADIX, H.J., "Self-compacting concrete: the role of the particle size distribution", In: *Proceedings of the 1st International Symposium on Design, Performance and Use of SCC*, pp. 109–118, Hunan, China, 2005. doi: https://doi.org/10.1617/2912143624.010.

[47] KAY, A., FREASON, J., "An investigation into the use of dune sand in concrete", In: *Proceedings of the 1st International Symposium on Engineering Characteristics of Arid Soils*, pp. 261–672, 1994.

[48] OUZIANI, T., ABDELBAKI, B., MADANI, B., *et al.*, "Effect of marble powder on the properties of self-compacting sand concrete", *The Open Construction & Building Technology Journal*, v. 5, n. 1, pp. 25–29, 2011. doi: https://doi.org/10.2174/1874836801105010025.

[49] BOUZIANI, T., BEDERINA, M., HADJOUDJA, M., "Effect of dune sand on the properties of flowing sand-concrete (FSC)", *International Journal of Concrete Structures and Materials*, v. 6, n. 1, pp. 59–64, 2012. doi: https://doi.org/10.1007/s40069-012-0006-z.

[50] BOUZIANI, T., "Assessment of fresh properties and compressive strength of self-compacting concrete made with different sand types by mixture design modelling approach", *Construction & Building Materials*, v. 49, pp. 308–314, 2013. doi: https://doi.org/10.1016/j.conbuildmat.2013.08.039.

[51] BOUZIANI, T., BEDERINA, M., MAKHLOUFI, Z., *et al.*, "Mixture design approach to evaluate fresh properties of SCC made with various sands", *Journal of Building Materials and Structures*, v. 1, n. 1, pp. 1–9, 2014. doi: https://doi.org/10.34118/jbms.v1i1.3.

[52] BOUZIANI, T., BENMOUNAH, A., MAKHLOUFI, Z., *et al.*, "Properties of flowable sand concretes reinforced by polypropylene fibers", *Journal of Adhesion Science and Technology*, v. 28, n. 18, pp. 1823–1834, 2014. doi: https://doi.org/10.1080/01694243.2014.924176.

[53] RMILI, A., BEN OUEZDOU, M., ADDED, M., *et al.*, "Incorporation of crushed sands and Tunisian desert sands in the composition of self compacting concretes. Part II: SCC fresh and hardened states characteristics", *International Journal of Concrete Structures and Materials*, v. 3, n. 1, pp. 11–14, 2009. doi: https://doi.org/10.4334/IJCSM.2009.3.1.011.

[54] GOUPY, J., "Les plans d'experiences" [Design of experiments], *Revue MODULAD*, n. 34, 2006.

[55] SEYED, M., BEDERINA, M., MAKHLOUFI, Z., "Effect of ternary binder on the mechanical and microstructural properties of sand concrete", *Journal of Adhesion Science and Technology*, v. 30, n. 4, pp. 339–361, 2016. doi: https://doi.org/10.1080/01694243.2015.1099867.

[56] SAHRAOUI, M., BOUZIANI, T., "Effects of fine aggregates types and contents on rheological and fresh properties of SCC", *Journal of Building Engineering*, v. 26, pp. 100890, 2019. doi: https://doi.org/10.1016/j.jobe.2019.100890.

[57] TIPU, R.K., GOYAL, A., SINGH, D., *et al.*, "Integrated deep learning and Bayesian optimization approach for enhanced prediction of high-performance concrete strength", *Asian Journal of Civil Engineering*, v. 26, n. 6, pp. 2371–2390, 2025. doi: https://doi.org/10.1007/s42107-025-01313-y.

[58] TIPU, R.K., ARORA, R., KUMAR, K., "Machine learning-based prediction of concrete strength properties with coconut shell as partial aggregate replacement: A sustainable approach in construction engineering", *Asian Journal of Civil Engineering*, v. 25, n. 3, pp. 2979–2992, 2024a. doi: https://doi.org/10.1007/s42107-023-00957-y.

[59] TIPU, R.K., BATRA, V., SUMAN, R., *et al.*, "Optimizing compressive strength in sustainable concrete: a machine learning approach with iron waste integration", *Asian Journal of Civil Engineering*, v. 25, n. 6, pp. 4487–4512, 2024b. doi: https://doi.org/10.1007/s42107-024-01061-5.

[60] TIPU, R.K., PANCHAL, V., PANDYA, K., "Multi-objective optimized high-strength concrete mix design using a hybrid machine learning and metaheuristic algorithm", *Asian Journal of Civil Engineering*, v. 24, n. 3, pp. 849–867, 2023. doi: https://doi.org/10.1007/s42107-022-00535-8.

[61] BOGUE, R.H., *Chemistry of Portland cement*, 2 ed., New York, Reinhold Publishing Corp, 1955.

[62] GOUPY, J., CREIGHTON, L., *Introduction to design of experiments with JMP examples*, 3 ed., Cary, SAS Institute, 2007.

[63] MEZGHICHE, B., *Laboratory testing of construction materials*, Algerie, Universitaire Biskra, 2005.

[64] ASSOCIATION FRANÇAISE DE NORMALISATION, *NF P 18-451* Béton frais - Essai d'affaissement au cône, Paris, AFNOR, 1981.

[65] ASSOCIATION FRANÇAISE DE NORMALISATION, *NF P18-459 Concrete - Test for Hardened Concrete - Porosity and Density Test*, Paris, AFNOR, 2022.

[66] ASSOCIATION FRANÇAISE DE NORMALISATION, *NF EN 12390-5, Essais Pour Béton Durci - Partie 5: Résistance a la Flexion sur Éprouvettes* Paris, AFNOR, 2012.

[67] AFPC-AFREM, "Recommended methods for measuring magnitudes associated with durability ", In: *Proceedings of the AFPC-AFREM Technical Days "Durability of Concretes"*, pp. 153–158, Toulouse, 1997.

[68] ASSOCIATION FRANÇAISE DE NORMALISATION, *NF EN 12390-3 Essais Pour Béton Durci - Partie 3: Résistance a la Compression des Éprouvettes*, Paris, AFNOR, 2012.

[69] AMERICAN SOCIETY FOR TESTING AND MATERIALS, ASTM C597-02 *Standard Test Method for Pulse Velocity Through Concrete*, West Conshohocken, ASTM, v. 4, 2002.

[70] RABEHI, M., MEZGHICHE, B., GUETTALA, S., "Correlation between initial absorption of the cover concrete, the compressive strength and carbonation depth", *Construction & Building Materials*, v. 45, pp. 123–129, 2013. doi: https://doi.org/10.1016/j.conbuildmat.2013.03.074.

[71] RABEHI, M., GUETTALA, S., MEZGHICHE, B., "The open porosity of the cover concrete: correlation between compressive strength and initial absorption", *European Journal of Environmental and Civil Engineering*, v. 16, n. 6, pp. 730–743, 2012. doi: https://doi.org/10.1080/19648189.2012.675174.

[72] CHETBANI, Y., BOUMAAZA, M., ZAITRI, R., *et al*., "Study of the effect of hemp fibers and brick waste powder on the mechanical characteristics of mortar: experimental and statistical analysis", *Journal of Natural Fibers*, v. 22, n. 1, pp. 2438900, 2025. doi: https://doi.org/10.1080/15440478.2024.2438900.

[73] RAOUACHE, E., BOUMAAZA, M., CHETBANI, Y., *et al*., "Shearing behavior of short high-performance concrete beams reinforced with swimmer bars: experimental and statistical studies", *European Journal of Environmental and Civil Engineering*, v. 29, n. 9, pp. 1912–1934, 2025. doi: https://doi.org/10.1080/19648189.2025.2464005.

[74] BERTINETTO, C., ENGEL, J., JANSEN, J., "ANOVA simultaneous component analysis: a tutorial review", *Analytica Chimica Acta: X*, v. 6, pp. 100061, 2020. doi: https://doi.org/10.1016/j.acax.2020.100061. PubMed PMID: 33392497.

[75] NANDA, A., MOHAPATRA, B.B., MAHAPATRA, A.P.K., *et al*., "Multiple comparison test by Tukey's honestly significant difference (HSD): do the confident level control type I error", *International Journal of Statistics and Applied Mathematics*, v. 6, n. 1, pp. 59–65, 2021. doi: https://doi.org/10.22271/maths.2021.v6.i1a.636.

[76] KUMAR, R., "Modified mix design and statistical modelling of lightweight concrete with high volume micro fines waste additive via the Box-Behnken design approach", *Cement and Concrete Composites*, v. 113, pp. 103706, 2020. doi: https://doi.org/10.1016/j.cemconcomp.2020.103706.

[77] SINKHONDE, D., "Generating response surface models for optimisation of CO_2 emission and properties of concrete modified with waste materials", *Clean. Mater.*, v. 6, pp. 100146, 2022. doi: https://doi.org/10.1016/j.clema.2022.100146.

[78] ROUT, M.K.D., SHUBHAM, K., BISWAS, S., *et al*., "An integrated evaluation of waste materials containing recycled asphalt fine aggregates using central composite design", *Asian Journal of Civil Engineering*, v. 25, n. 1, pp. 1007–1025, 2024. doi: https://doi.org/10.1007/s42107-023-00828-6.

[79] BUREAU OF INDIAN STANDARDS, *IS 13311-1 Method of non-destructive testing of concrete, Part 1: Ultrasonic pulse velocity - CED 2: Cement and Concrete*, New Delhi, BIS, 1992.

[80] AWOLUSI, T.F., OKE, O.L., AKINKUROLERE, O.O., *et al*., "Application of response surface methodology: predicting and optimizing the properties of concrete containing steel fibre extracted from waste tires with limestone powder as filler", *Case Studies in Construction Materials*, v. 10, e00212, 2019. doi: https://doi.org/10.1016/j.cscm.2018.e00212.

[81] BOUMAAZA, M., BELAADI, A., BOURCHAK, M., *et al*., "Comparative study of flexural properties prediction of Washingtonia filifera rachis biochar bio-mortar by ANN and RSM models", *Construction & Building Materials*, v. 318, pp. 125985, 2022. doi: https://doi.org/10.1016/j.conbuildmat.2021.125985.

[82] ABDULKADIR, I., MOHAMMED, B.S., "RSM analysis and study on the 6 months compressive strength development and shrinkage behaviour of high volume fly ash rubberized ECC (HVFA-RECC)", *International Journal of Advanced Research in Engineering and Technology*, v. 11, pp. 965–980, 2020.

[83] DEMIRBOĞA, R., TÜRKMEN, İ., KARAKOÇ, M.B., "Relationship between ultrasonic velocity and compressive strength for high-volume mineral-admixtured concrete", *Cement and Concrete Research*, v. 34, n. 12, pp. 2329–2336, 2004. doi: https://doi.org/10.1016/j.cemconres.2004.04.017.

[84] OMRANE, M., RABEHI, M., "Effect of natural pozzolan and recycled concrete aggregates on thermal and physico-mechanical characteristics of self-compacting concrete", *Construction & Building Materials*, v. 247, pp. 118576, 2020. doi: https://doi.org/10.1016/j.conbuildmat.2020.118576.